CHAPTER

Magnetic Ordering

13

CHAPTER OUTLINE

Physics of Condensed Matter. DOI: 10.1016/B978-0-12-384954-0.00013-X

13.1 INTRODUCTION

The phenomena of magnetic ordering such as ferromagnetism, antiferromagnetism, and ferrimagnetism are very complex. Ferromagnets have been known to exist for thousands of years in the shape of loadstones. However, ferromagnetism in transition metals, which is one of the most important as well as complex phenomena in physics, remains one of the major unsolved problems in solid state physics and is not well understood compared to most other physical properties. We will discuss some of the important models used in the theory of magnetic ordering used in solids before discussing some specific cases, including that of ferromagnetism in transition metals.

There are three different types of "magnetic ordering," known as ferromagnetism, antiferromagnetism, and ferrimagnetism. The ferromagnetic solid has a nonvanishing magnetic moment even in the absence of an external magnetic field. This is known as "spontaneous magnetization," which is a result of parallel orientation of the individual magnetic moments that must be due to interactions between these moments. In a ferromagnet, because all the individual moments are aligned in the same direction, there is a net total moment even in the absence of a magnetic field. As the temperature is increased, these orientations become gradually disordered, and at a critical temperature known as the Curie temperature, the spontaneous magnetization vanishes. This situation is far more complicated than the simple model used at $T = 0$. In the preceding discussion, we tacitly assumed that the electrons of an ion in a lattice are tightly bound so that each ion has a net magnetic moment.

In some other types of solids, the ions of the nearest neighbors have antiparallel spin. The ground state consists of two sublattices of identical ions having opposite spin directions. This is known as an antiferromagnet, in which the two sublattices have mutually compensating magnetic moments. Thus, the net magnetic moment of an antiferromagnet is zero.

In ferrimagnets, there are usually two types of basis atoms and therefore two sublattices because the ions in the individual sublattices are different. The individual ions in each sublattice will possess a magnetic moment, and each sublattice will have a net magnetic moment in the ground state. The total moment in the ground state will be the vector sum of the moments of the sublattices. For sublattices with opposite magnetic moments, the net magnetic moment will be the difference between the two moments. Such types of solids are known as ferrimagnets. These differences are illustrated in Figure 13.1.

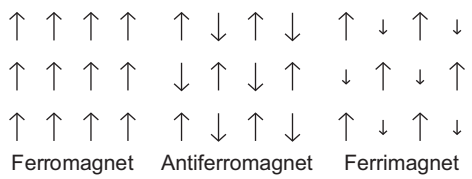

FIGURE 13.1
Ferromagnetic, antiferromagnetic, and ferrimagnetic states.

13.2 MAGNETIC DIPOLE MOMENTS

The simplest problem involves magnetic dipole moments and how nearby magnetic dipoles interact with each other even though such interaction does not lead to ferromagnetism.

The magnetic dipole moment $\mathbf{m}$ of a current distribution $\mathbf{j}$ can be defined as

$$\mathbf{m} = \int d\mathbf{r}\, \frac{1}{2c}\mathbf{r}\times\mathbf{j}(\mathbf{r}). \tag{13.1}$$

We note that $\mathbf{m}$ will be independent of the origin provided $\int d\mathbf{r}\, \mathbf{j}(\mathbf{r}) = 0$, which implies that the current distribution is over a closed loop and vanishes except at the origin. The Lorentz force on a current distribution is

$$\mathbf{F} = \frac{1}{c}\int d\mathbf{r}\, \mathbf{j}(\mathbf{r})\times\mathbf{B}(\mathbf{r}). \tag{13.2}$$

Because $\mathbf{j}(\mathbf{r})$ vanishes except at the origin, we can expand $\mathbf{B}(\mathbf{r})$ in a Taylor series and write

$$\mathbf{F} = \frac{1}{c}\int d\mathbf{r}\, \mathbf{j}(\mathbf{r})\times[\mathbf{B}(0) + (\mathbf{r}\cdot\overrightarrow{\nabla})\mathbf{B}(0) + \cdots]. \tag{13.3}$$

Using vector identities, we can easily show from Eqs. (13.1) through (13.3) that (Problem 13.1)

$$\mathbf{F} = (\mathbf{m}\times\overrightarrow{\nabla})\times\mathbf{B} = \overrightarrow{\nabla}(\mathbf{m}\cdot\mathbf{B}), \tag{13.4}$$

where $\mathbf{B}\equiv\mathbf{B}(0)$. Thus, the potential energy U of a dipole in an external magnetic field is

$$U = -\mathbf{m}\cdot\mathbf{B}. \tag{13.5}$$

When two dipoles are close to each other, they interact with each other's magnetic fields.

The induction $\mathbf{B}$ produced by a magnetic dipole of moment $\mathbf{m}_1$ at a distance $\mathbf{r}$, where a second dipole of moment $\mathbf{m}_2$ is located, is given by

$$\mathbf{B} = \overrightarrow{\nabla}\left[\mathbf{m}_1\cdot\overrightarrow{\nabla}\frac{1}{r}\right] = \frac{3\hat{\mathbf{r}}(\mathbf{m}_1\cdot\hat{\mathbf{r}}) - \mathbf{m}_1}{r^3}. \tag{13.6}$$

From Eqs. (13.5) and (13.6), we obtain the expression for the direct dipolar interaction energy of two magnetic dipoles separated by $\mathbf{r}$,

$$U = \frac{1}{r^3}[\mathbf{m}_1\cdot\mathbf{m}_2 - 3(\mathbf{m}_1\cdot\hat{\mathbf{r}})(\mathbf{m}_2\cdot\hat{\mathbf{r}})]. \tag{13.7}$$

One can calculate the energy scale for the dipole interaction from Eq. (13.7), which is of the order of 10^{-4} eV (equivalent to 1° K) for solids in which the distance between magnetic moments is of the order of 2 Å, while the electrostatic energy difference between two atomic states is on the order of 0.1–1.0 eV. Thus, dipolar interactions, which are important in explaining the phenomenon of ferromagnetic domains, are not the source of magnetic interaction responsible for ferromagnetism.

13.3 MODELS FOR FERROMAGNETISM AND ANTIFERROMAGNETISM

13.3.1 Introduction

Various models describe ferromagnetism and antiferromagnetism. The direct exchange model assumes that the electrons of a lattice ion, which contribute to the magnetic moment, are tightly bound so that the ions can be assumed to be isolated. However, the nearest neighbors are sufficiently close enough for a significant exchange interaction between them. The spins of nearest neighbors in the Bravais lattice of a ferromagnet (where electrons are tightly bound in the lattice ion) are aligned parallel in the ground state by the exchange interaction. In the absence of such interactions, the moments would be thermally disordered due to random orientations, and there would be no magnetic moment.

In the superexchange model, an exchange between magnetic ions occurs over large distances in an insulator, in which a paramagnetic ion between them facilitates the interaction. An example is MnO, in which two metallic ions (Mn) with unfilled *d*-shells are linked by an oxygen atom that has two *p*-electrons with spins in opposite directions. Each *d*-electron will interact with one of the two *p*-electrons, and because the two *p*-electrons are linked by the Pauli principle, there is an effective interaction between the two *d*-electrons that is known as the superexchange.

In the indirect exchange (RKKY) model (Refs. 10, 23, 31), the localized spins of a lattice ion interact with the conduction electrons of a metal. Essentially, the electrons mediate between the interaction of the lattice ions. This ion–ion interaction via conduction electrons plays a major role in rare-earth metals, which have a variety of ordered magnetism.

In the transition metals, which form the most significant group of ferromagnetic metals, the spins of itinerant electrons give rise to ferromagnetism. The *d*- and *s*-bands are only partly filled, and hence, there is a superposition of $3d$ and $4s$ bands. We will discuss the occurrence of ferromagnetism in transition metals as a special category.

13.3.2 Heitler–London Approximation

The Heitler–London (Ref. 6) approximation is designed to describe the interaction between two spins arising from Coulomb forces between the two electrons of two adjacent atoms, as shown in Figure 13.2. It was originally designed to explain the bonding of a hydrogen molecule and is also an example of the valence bond method. We further note that the Heitler–London theory does not yield good results for the binding energy of the hydrogen molecule. The reason is that when two protons are close, the system looks like the helium atom with $Z = 2$, whereas in the Heitler–London theory, the electrons are in *s* states for $Z = 1$. However, it features the essential ingredients of the exchange

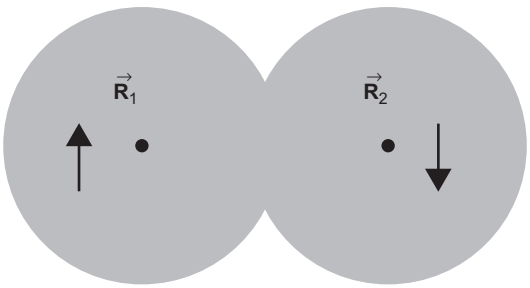

FIGURE 13.2

The overlapping wave functions of electrons (of opposite spin) of two adjacent hydrogen atoms. The protons are located at $\vec{R}_1$ and $\vec{R}_2$. The arrows are the directions of the spins of the electrons.

interaction used in the theory of magnetism in insulators, and hence, we will discuss the theory in some detail.

When the two hydrogen atoms ($i=1$ and $i=2$) are infinitely apart, the Schrodinger equation for each atom can be written as

$$\left[-\frac{\hbar^2\nabla_i^2}{2m}-\frac{e^2}{|\mathbf{r}_i-\mathbf{R}_i|}\right]\phi_i(\mathbf{r}_i)=\varepsilon_0\phi_i(\mathbf{r}_i), \tag{13.8}$$

which is the spatial part of the wave function. The wave function of the two atoms is just the product of the individual atomic wave functions. When the two atoms come much closer, there will be considerable overlap, and a molecule is formed. The individual atomic wave functions will not be orthogonal. In fact,

$$\int \phi_1^*(\mathbf{r})\phi_2(\mathbf{r})d\mathbf{r}=I, \tag{13.9}$$

where I is the overlap integral, which can be positive or negative. The Hamiltonian can be written as

$$\hat{H}=\frac{-\hbar^2\nabla_1^2}{2m}-\frac{\hbar^2\nabla_2^2}{2m}-\frac{e^2}{|\mathbf{r}_1-\mathbf{R}_1|}-\frac{e^2}{|\mathbf{r}_1-\mathbf{R}_2|}-\frac{e^2}{|\mathbf{r}_2-\mathbf{R}_1|}-\frac{e^2}{|\mathbf{r}_2-\mathbf{R}_2|}+\frac{e^2}{|\mathbf{R}_1-\mathbf{R}_2|}+\frac{e^2}{|\mathbf{r}_1-\mathbf{r}_2|}. \tag{13.10}$$

Here, the electrostatic interactions between the two electrons and the two protons, with all permutations, have been included in the Hamiltonian of the molecule. It may be noted that the wave function of the molecule is no longer the product of the individual atomic functions. The spin component of the wave function has to be included such that the total wave function will be antisymmetric when the particle numbers are exchanged. The spin operators commute with the spatial part of the Hamiltonian. The spin eigenfunctions are the eigenfunctions of the commuting operators $\hat{S}^2$ and $\hat{S}_z$ and form either one singlet or three triplet states. The spin singlet state of the molecule is given by

$$\chi_s=\frac{1}{\sqrt{2}}[\chi_\uparrow(1)\chi_\downarrow(2)-\chi_\downarrow(1)\chi_\uparrow(2)], \tag{13.11}$$

which is antisymmetric, and the three-spin triplet states are

$$\begin{aligned}\chi_t&=\chi_\uparrow(1)\chi_\uparrow(2),\\&=\frac{1}{\sqrt{2}}[\chi_\uparrow(1)\chi_\downarrow(2)+\chi_\downarrow(2)\chi_\uparrow(1)],\\&=\chi_\downarrow(1)\chi_\downarrow(2),\end{aligned} \tag{13.12}$$

which are all symmetric. Here, the symbols in the parentheses denote the spinors for the electrons at $\mathbf{r}_1$ and $\mathbf{r}_2$. Thus, the normalized spatial part of the wave functions of the singlet and triplet spin states are

$$\psi_{s,t}(\mathbf{r}_1,\mathbf{r}_2)=[2(1\pm I^2)]^{-\frac{1}{2}}[\phi_1(\mathbf{r}_1)\phi_2(\mathbf{r}_2)\pm\phi_2(\mathbf{r}_1)\phi_1(\mathbf{r}_2)], \tag{13.13}$$

where the s,t symbols as well as the $+(-)$ signs are for the singlet (triplet) spin states.

From Eqs. (13.8) through (13.10) and Eq. (13.13), we obtain (Problem 13.3)

$$\varepsilon_{s,t}=<\hat{H}>_{s,t}=2\varepsilon_0+\frac{e^2}{R_{12}}+e^2\int d\mathbf{r}_1 d\mathbf{r}_2\,\psi_{s,t}^*(\mathbf{r}_1,\mathbf{r}_2)\left[\frac{1}{|\mathbf{r}_1-\mathbf{r}_2|}-\frac{1}{|\mathbf{r}_1-\mathbf{R}_2}-\frac{1}{|\mathbf{r}_2-\mathbf{R}_1|}\right]\psi_{s,t}(\mathbf{r}_1,\mathbf{r}_2), \tag{13.14}$$

where

$$\frac{1}{R_{12}} \equiv \frac{1}{|\mathbf{R}_1 - \mathbf{R}_2|}. \tag{13.15}$$

We define the Coulomb and exchange integrals as

$$V_c(R_{12}) = e^2 \int d\mathbf{r}_1 d\mathbf{r}_2 |\phi_1(\mathbf{r}_1)|^2 |\phi_2(\mathbf{r}_2)|^2 \left[\frac{1}{|\mathbf{r}_1 - \mathbf{r}_2|} - \frac{1}{|\mathbf{r}_1 - \mathbf{R}_1|} - \frac{1}{|\mathbf{r}_2 - \mathbf{R}_2|}\right] \tag{13.16}$$

and

$$V_{ex}(R_{12}) = e^2 \int d\mathbf{r}_1 d\mathbf{r}_2 \phi_1^*(\mathbf{r}_1)\phi_2^*(\mathbf{r}_2) \left[\frac{1}{|\mathbf{r}_1 - \mathbf{r}_2|} - \frac{1}{|\mathbf{r}_1 - \mathbf{R}_2|} - \frac{1}{|\mathbf{r}_2 - \mathbf{R}_1|}\right] \phi_2(\mathbf{r}_1)\phi_1(\mathbf{r}_2). \tag{13.17}$$

From Eqs. (13.14) through (13.17), it can be shown that (Problem 13.4)

$$\varepsilon_s = 2\varepsilon_0 + \frac{e^2}{R} + \frac{V_c(R_{12}) + V_{ex}(R_{12})}{(1 + I^2)} \tag{13.18}$$

and

$$\varepsilon_t = 2\varepsilon_0 + \frac{e^2}{R} + \frac{V_c(R_{12}) - V_{ex}(R_{12})}{(1 - I^2)}. \tag{13.19}$$

From Eqs. (13.18) and (13.19), we obtain

$$\varepsilon_t - \varepsilon_s = \frac{2(I^2 V_e - V_s)}{1 - I^4} = -J. \tag{13.20}$$

Heitler and London (Ref. 6) found that J is negative, which implies that $\varepsilon_t > \varepsilon_s$. Because the singlet state is of lower energy, the spins of the two atoms are in opposite directions, which is an example of two-atom antiferromagnetism.

13.3.3 Spin Hamiltonian

Dirac and Heisenberg argued that the original Hamiltonian in Eq. (13.10) acts only on the spatial degrees of freedom and yields two eigenvalues, ε_s and ε_t (one singlet and three degenerate triplet states, depending on whether the spins of the two electrons are parallel or antiparallel). They showed that the same results can be obtained by considering a Hamiltonian that involves only the spin degrees of freedom and that is more useful in the study of magnetism.

The actual wave function of the Heitler–London problem (Ref. 6) is the product of the spin (Eqs. 13.11 or 13.12) and spatial part of the wave function (Eq. 13.13), i.e.,

$$\Psi_s = \psi_s \chi_s \tag{13.21}$$

and

$$\Psi_t = \psi_t \chi_t. \tag{13.22}$$

It is much more convenient to represent the Hamiltonian in a spin representation as long as the energy in the singlet (ε_s) and triplet (ε_t) states derived in Eqs. (13.18) and (13.19) by using the

spatial Hamiltonian of the two-electron system are the same in the new representation. This is possible because the coupling in the spin Hamiltonian depends only on the relative orientation of the two spins but not on their directions on $\mathbf{R}_1 - \mathbf{R}_2$. If there are dipolar interactions or spin-orbit coupling, which breaks the rotational symmetry of the Hamiltonian in the Heitler–London model, one must add additional terms to the spin Hamiltonian. Thus, the spin Hamiltonian can be written as

$$\hat{H}^{spin} = \lambda_1 + \lambda_2 \hat{\mathbf{S}}_1 \cdot \hat{\mathbf{S}}_2, \tag{13.23}$$

where λ_1 and λ_2 are such that

$$\hat{H}^{spin} \Psi_s = \varepsilon_s \Psi_s \tag{13.24}$$

and

$$\hat{H}^{spin} \Psi_t = \varepsilon_t \Psi_t. \tag{13.25}$$

We also note that for a two-electron system,

$$\hat{\mathbf{S}}_1 \cdot \hat{\mathbf{S}}_2 = \frac{1}{2}[\hat{S}_1^+ \hat{S}_2^- + \hat{S}_2^+ \hat{S}_1^-] + \hat{S}_1^z \hat{S}_2^z, \tag{13.26}$$

where

$$\hat{S}^{\pm} = \hat{S}_x \pm i\hat{S}_y. \tag{13.27}$$

It can be easily shown from Eqs. (13.11), (13.12), and (13.24) through (13.26) that (Problem 13.5)

$$\hat{\mathbf{S}}_1 \cdot \hat{\mathbf{S}}_2 \chi_s = -\frac{3}{4}\chi_s \tag{13.28}$$

and

$$\hat{\mathbf{S}}_1 \cdot \hat{\mathbf{S}}_2 \chi_t = \frac{1}{4}\chi_t. \tag{13.29}$$

From Eqs. (13.24) through (13.29), we obtain

$$\hat{H}^{spin} = \frac{1}{4}(\varepsilon_s + 3\varepsilon_t) - (\varepsilon_s - \varepsilon_t)\hat{\mathbf{S}}_1 \cdot \hat{\mathbf{S}}_2, \tag{13.30}$$

such that

$$\hat{H}^{spin} \Psi_s = \varepsilon_s \Psi_s \tag{13.31}$$

and

$$\hat{H}^{spin} \Psi_t = \varepsilon_t \Psi_t \tag{13.32}$$

for each of the three triplet states. Comparing Eqs. (13.23) and (13.30), we obtain

$$\lambda_1 = \frac{1}{4}(\varepsilon_s + 3\varepsilon_t) \tag{13.33}$$

and

$$\lambda_2 = (\varepsilon_s - \varepsilon_t). \tag{13.34}$$

From Eqs. (13.18) through (13.20), (13.23), (13.33), and (13.34), we obtain

$$\hat{H}^{spin} = 2\varepsilon_0 + \frac{e^2}{R} + \frac{1}{4}\left[\frac{V_c(R_{12}) + V_{ex}(R_{12})}{1+I^2} + 3\frac{V_c(R_{12} - V_{ex}(R_{12})}{1-I^2}\right] - J\hat{\mathbf{S}}_1 \cdot \hat{\mathbf{S}}_2. \tag{13.35}$$

By shifting the zero of energy, we can rewrite Eq. (13.35) in the convenient form

$$\hat{H}^{spin} = -J\hat{\mathbf{S}}_1 \cdot \hat{\mathbf{S}}_2. \tag{13.36}$$

Because $J = \varepsilon_s - \varepsilon_t$ (from Eq. 13.20), a positive value of J means that $\varepsilon_t < \varepsilon_s$. This implies that the two spins are aligned in the same direction (ferromagnetism). Similarly, a negative value of J implies that the spins are aligned in the opposite direction. This alternate change in the direction of the spins is known as antiferromagnetism.

13.3.4 Heisenberg Model

Heisenberg (Ref. 5) extended Eq. (13.36) for the general case of a large collection of magnetic ions placed in a lattice. He postulated that the Hamiltonian can be written as

$$\hat{H}^{spin} = -\sum_{ij}{}' J_{ij}\hat{\mathbf{S}}_i \cdot \hat{\mathbf{S}}_j, \tag{13.37}$$

where the exchange integral J_{ij} is a function of the positions of the lattice sites $\mathbf{R}_i$ and $\mathbf{R}_j$ (note that $\mathbf{R}_i \neq \mathbf{R}_j$). We further note that the exchange integral J_{ij}, which is a function of $\mathbf{R}_i - \mathbf{R}_j$, is large only for one- or two-lattice spacing. It is not possible to "derive" the Heisenberg Hamiltonian, but there have been many attempts to "derive" it or at least make reasonable attempts to justify it. Nevertheless, it remains the starting point for the theory of ferromagnetism and antiferromagnetism.

13.3.5 Direct, Indirect, and Superexchange

The Heisenberg model is the result of the direct overlap of wave functions of two magnetic ions. This is due to the direct exchange interaction between localized spins of nearest neighbors, and the basic assumption is that the electrons (of a lattice ion) are tightly bound such that the ion can be considered as isolated, but the nearest neighbors are close enough for exchange interaction to occur.

However, there are other mechanisms for exchange. In indirect exchange, the localized spins of the lattice ions interact with the conduction electrons of a metal. Thus, the information on the spin over a given ion is passed on by an electron to another ion. Hence, the interaction between the two ions is mediated by conduction electrons. This indirect ion–ion interaction is known as the RKKY interaction (Refs. 10, 20, 23) and plays a major role in the rare-earth metals (Tm and Gd).

In the superexchange mechanism in an insulator, the exchange between magnetic ions often occurs over large distances. A paramagnetic ion (an ion with closed electronic shells) between the two magnetic ions facilitates the interaction. For example, in MnO, two metallic ions with unfilled d-shells are linked by an oxygen atom. Each d-electron interacts with one of the two p-electrons of the spin-saturated outermost electron pair of the oxygen atom. There is an effective interaction between the two d-electrons, known as superexchange, because the two spins of the two p-electrons

are linked by the Pauli principle. These three types of interactions are shown schematically in Figure 13.3.

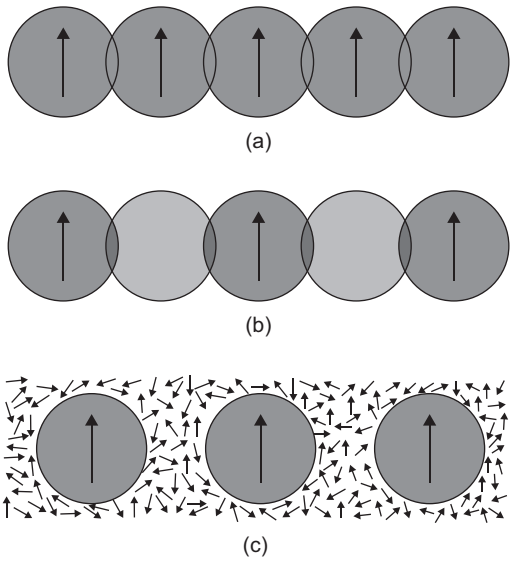

FIGURE 13.3
(a) Direct exchange, (b) superexchange, and (c) indirect exchange.

13.3.6 Spin Waves in Ferromagnets: Magnons

For ferromagnets, the ground state of the Heisenberg model is such that all the J_{ij} are positive and all the spins point in the same direction. It can be easily shown from Eq. (13.35) that if all the spins point in the same direction (for instance, z), the ground-state energy is

$$<\uparrow\uparrow\uparrow\uparrow \cdots |\hat{H}|\uparrow\uparrow\uparrow\uparrow \cdots ...> = -\sum_{<ii'>}{}' \frac{J_{ii'}}{4}. \tag{13.38}$$

The ferromagnetic state of the ground state is degenerate. Even though the spins have to point in the same direction, there is no preference for a particular direction like z direction. The low-energy excitons can be constructed by slowly twisting the local spin orientation while propagating through the crystal. These propagations are known as spin waves.

13.3.7 Schwinger Representation

We note that in an excited state, the spin of one or more ions at a lattice site is reversed from ↑ to ↓. Each time such a spin reversal occurs, the net spin change is 1. Thus, the appropriate operators to represent such changes are Bose operators. Schwinger (Ref. 24) proposed a formal theory of spin waves by using a representation in which the spins are represented by Bose operators even though the Heisenberg Hamiltonian is a product of Fermion operators. In this representation, the Bose operators are defined as

$$\hat{S}^{\alpha} = \frac{1}{2}\sum_{ij} \hat{a}_i^{\dagger}\sigma_{ij}^{\alpha}\hat{a}_j, \tag{13.39}$$

where σ^{α} are the Pauli spin matrices ($\alpha = x, y, z$). It is easy to show from Eq. (13.39) that (Problem 13.6)

$$\begin{aligned} \hat{S}^{x} &= \frac{1}{2}(\hat{a}_1^{\dagger}\hat{a}_2 + \hat{a}_2^{\dagger}\hat{a}_1), \\ \hat{S}^{y} &= \frac{i}{2}(\hat{a}_2^{\dagger}\hat{a}_1 - \hat{a}_1^{\dagger}\hat{a}_2), \text{ and} \\ \hat{S}^{z} &= \frac{1}{2}(\hat{a}_1^{\dagger}\hat{a}_1 - \hat{a}_2^{\dagger}\hat{a}_2). \end{aligned} \tag{13.40}$$

It can be easily shown from Eq. (13.40) that

$$[\hat{S}^x, \hat{S}^y] = i\hat{S}^z. \tag{13.41}$$

If one introduces the operators

$$\hat{S}^{\pm} = \hat{S}^x \pm i\hat{S}^y, \tag{13.42}$$

it can be shown from Eqs. (13.40) and (13.42) that

$$\hat{S}^+ = \hat{a}_1^\dagger \hat{a}_2 \tag{13.43}$$

and

$$\hat{S}^- = \hat{a}_2^\dagger \hat{a}_1. \tag{13.44}$$

Because the total spin is $2S$, one can write

$$\hat{a}_1^\dagger \hat{a}_1 + \hat{a}_2^\dagger \hat{a}_2 = 2S. \tag{13.45}$$

Through use of the Holstein–Primakoff transformation (Ref. 7) (which is an unusual transformation to be used for operators, but seems to be valid), Eq. (13.45) becomes

$$\hat{a}_2 = \sqrt{2S - \hat{a}_1^\dagger \hat{a}_1}. \tag{13.46}$$

From Eqs. (13.40) and (13.46), we obtain

$$\begin{aligned} \hat{S}^+ &= \hat{a}_1^\dagger \sqrt{2S - \hat{a}_1^\dagger \hat{a}_1}, \\ \hat{S}^- &= \sqrt{2S - \hat{a}_1^\dagger \hat{a}_1}\, \hat{a}_1, \text{ and} \\ \hat{S}^z &= (\hat{a}_1^\dagger \hat{a}_1 - S). \end{aligned} \tag{13.47}$$

One can easily show that (Problem 13.7)

$$[\hat{S}^+, \hat{S}^-] = 2\hat{S}^z. \tag{13.48}$$

13.3.8 Application to the Heisenberg Hamiltonian

If we assume that the direct exchange interaction between the nearest neighbors is dominant, for simple lattices, Eq. (13.37) can be rewritten as

$$\hat{H} = -J \sum_{i,\delta}{}' \hat{\mathbf{S}}_i \cdot \hat{\mathbf{S}}_{i+\delta}, \tag{13.49}$$

where $\mathbf{R}_j = \mathbf{R}_i + \mathbf{R}_\delta$, $\mathbf{R}_\delta\,(\delta = 1, 2, ..., z)$ is a vector to the nearest neighbor of the ith ion and $J_{i,i+\delta} = J$ for all δ. If J is positive in Eq. (13.49), it leads to ferromagnetism. The ion spins are assumed to be so aligned that in the ground state their z-components have the maximum values S. If $|S>_n$ represents the spin of the nth ion in state s, the ground state can be written as

$$\Phi_0 = \Pi_n |S>_n. \tag{13.50}$$

Eq. (13.49) can be rewritten in the alternate form

$$\hat{H} = -J\sum_{i,j}{}' \left[\hat{S}_{iz}\hat{S}_{jz} + \frac{1}{2}(\hat{S}_i^+ \hat{S}_j^- + \hat{S}_i^- \hat{S}_j^+)\right], \tag{13.51}$$

where $j = i + \delta$. Thus, we obtain

$$\hat{H}\Phi_0 = \varepsilon_0\Phi_0 = (-S^2 J \sum_{i,i+\delta} 1)\Phi_0 = -JS^2 zN\Phi_0, \tag{13.52}$$

where N is the total number of sites, z is the coordination number of each site, and the application of S^+ to a function with maximum spin leads to zero. Here, N is the total number of ions. Thus, we obtain the expression for the energy of the ground state for a ferromagnet,

$$\varepsilon_0 = -JNzS^2. \tag{13.53}$$

However, if we consider the state Φ_m in which the mth spin is reduced by 1, the new state can be written as

$$\Phi_m = \hat{S}_m^- \Pi_n |\, S >_n. \tag{13.54}$$

From Eqs. (13.51) and (13.54), we can write

$$\hat{H}\Phi_m = -J\sum_{ij}{}' \left[\hat{S}_i^z \hat{S}_j^z \hat{S}_m^- + \frac{1}{2}(\hat{S}_i^+ \hat{S}_j^- \hat{S}_m^- + \hat{S}_i^- \hat{S}_j^+ \hat{S}_m^-)\right]\Phi_0. \tag{13.55}$$

It can be easily shown by using the commutation relation of the spin operators (Problem 13.8) that

$$\hat{H}\Phi_m = E_0\Phi_m + 2JS\sum_{\mathbf{R}_\delta}(\Phi_m - \Phi_{m+\delta}). \tag{13.56}$$

Thus, Φ_m is not an eigenstate of the spin Hamiltonian. In fact, the deviation of spin at one site spreads into the neighboring sites, creating spin waves. To solve this, we take S to be large and expand in powers of $1/S$. For example, we obtain from Eqs. (13.47) and (13.51)

$$\begin{aligned}\hat{H} = -J\sum_{i,j}\Bigg[&(S - \hat{a}_i^\dagger \hat{a}_i)(S - \hat{a}_j^\dagger \hat{a}_j) + \frac{1}{2}\hat{a}_i^\dagger \sqrt{2S - \hat{a}_i^\dagger \hat{a}_i}\sqrt{2S - \hat{a}_j^\dagger \hat{a}_j}\,\hat{a}_j \\ &+ \frac{1}{2}\hat{a}_j^\dagger \sqrt{2S - \hat{a}_j^\dagger \hat{a}_j}\sqrt{2S - \hat{a}_i^\dagger \hat{a}_i}\,\hat{a}_i\Bigg],\end{aligned} \tag{13.57}$$

where $j = i + \delta$, δ being the nearest neighbors. For large values of S, we can write

$$\hat{a}_i = \sqrt{S}b_i + (\hat{a}_i - \sqrt{S}b_i), \tag{13.58}$$

where $(\hat{a}_i - \sqrt{S}b_i)$ is very small, and b_i is determined by minimizing the Hamiltonian. The constants b_i are determined by minimizing the Hamiltonian while the series in $1/S$ is obtained by expanding the remainder. Thus, Eq. (13.57) can be rewritten as

$$\hat{H} = -J\sum_{ij} S^2 \left[\frac{1}{2}(b_i^* b_j + b_j b_i^*)\sqrt{2 - |b_i|^2}\sqrt{2 - |b_j|^2} + (1 - |b_i|)^2(1 - |b_j|)^2\right]. \tag{13.59}$$

Here, it is tacitly assumed that i and j are nearest pairs. To obtain the ground-state energy, we minimize the Hamiltonian with respect to all values of b_i and b_j. The only possible way in which the

ground-state energy ε_0 obtained from Eq. (13.59) will be the same as obtained in Eq. (13.53) is to assume $b_i = b_j = b$ (Problem 13.9). In fact, if the spins rotate in any direction as long as they all point together, the ground-state energy is independent of b, which can therefore be chosen as $b = 0$. The operator $\hat{a}$ is treated as small (Eq. 13.58) if we continue with the expansion of the Hamiltonian.

From Eqs. (13.53) and (13.59), we can write $\hat{H}$ (up to the first order in S), treating $\hat{a}$ as small, $b = 0$, and multiplying the second term by 2 because $<ij>$ is a sum over nearest-neighbor pairs and each pair appears twice (Problem 13.10),

$$\hat{H} = -JNzS^2 - 2JS \sum_{<ij>} (\hat{a}_i^\dagger \hat{a}_j + \hat{a}_j^\dagger \hat{a}_i - \hat{a}_i^\dagger \hat{a}_i - \hat{a}_j^\dagger \hat{a}_j). \tag{13.60}$$

We make a Fourier transformation

$$\hat{a}_i = \frac{1}{\sqrt{N}} \sum_{\mathbf{k}} \hat{b}_{\mathbf{k}} e^{-i\mathbf{k}\cdot\mathbf{R}_i}, \tag{13.61}$$

where $\mathbf{k}$ (for cyclic boundary conditions) is limited to the N values inside a Brillouin zone in the $\mathbf{k}$ space. From Eqs. (13.60) and (13.61), we obtain

$$\hat{H} = -JNzS^2 + \sum_{\mathbf{k}} \hbar\omega_{\mathbf{k}} \hat{n}_{\mathbf{k}}, \tag{13.62}$$

where

$$\hat{n}_{\mathbf{k}} = \hat{b}_{\mathbf{k}}^\dagger \hat{b}_{\mathbf{k}} \tag{13.63}$$

and

$$\hbar\omega_{\mathbf{k}} = 2JS \sum_l (1 - \cos \mathbf{k} \cdot \mathbf{R}_l). \tag{13.64}$$

Eq. (13.64) gives the spin-wave dispersion relation. Here, $\mathbf{R}_l$ are the nearest neighbors. The first term in Eq. (13.64) is the energy of the ground state, the second term is the energy contained in the magnons, and $n_{\mathbf{k}} = \hat{b}_{\mathbf{k}}^\dagger \hat{b}_{\mathbf{k}}$ is the magnon particle number. The magnon energy can be expressed as

$$E = \sum_{\mathbf{k}} \frac{\hbar\omega_{\mathbf{k}}}{e^{\beta\hbar\omega_{\mathbf{k}}} - 1}, \tag{13.65}$$

where $\beta = 1/k_B T$. In the isotropic case, $\hbar\omega_{\mathbf{k}} \propto k^2 = \gamma k^2$ (from Eq. 13.65), and we obtain

$$E = \frac{V}{4\pi^3} \int_0^{k_{\max}} \frac{4\pi\gamma k^4 dk}{e^{\gamma k^2/k_B T} - 1}. \tag{13.66}$$

At very low temperatures, when only a few magnons are excited, the upper limit of the integration can be considered as infinity. Thus, Eq. (13.66) can be rewritten as

$$E = \frac{\gamma V}{\pi^2} \left(\frac{k_B T}{\gamma}\right)^{5/2} \int_0^\infty \frac{x^4 dx}{e^{x^2} - 1} = \alpha T^{5/2}, \tag{13.67}$$

where α is a constant. Thus, the specific heat is proportional to $T^{3/2}$, which agrees with the experimental results.

13.3.9 Spin Waves in Antiferromagnets

When J is negative in Eq. (13.49), the neighboring spins are aligned in opposite directions. If all the ions are of the same type, this leads to antiferromagnetism. In antiferromagnets, the neighboring spins are antiparallel at zero temperature; this is known as a Néel state (Ref. 21). The ground state of an antiferromagnet is schematically illustrated in Figure 13.4.

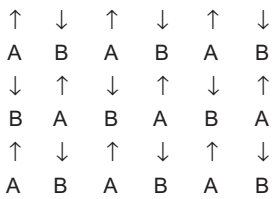

FIGURE 13.4
The spins are divided into two interpenetrating sublattices A and B in the Néel state.

The spin states can be described as two interpenetrating sublattices, A and B. Each spin state in A has spins in the B sublattice as the nearest neighbors. One way of solving the complicated problem is as follows. The spin Hamiltonian in the antiferromagnetic state can be obtained from that of the ferromagnetic state by rotating all the spin operators on the B sublattice by 180° about the x-axis, while keeping the spin operators intact in the A sublattice. Thus, $x \rightarrow x$, $y \rightarrow -y$, and $z \rightarrow -z$. If all the $\mathbf{R}_i$ vectors are in the A sublattice and the $\mathbf{R}_j$ vectors are in the B sublattice, the spin operators defined in Eqs. (13.40) and (13.42) for ferromagnets can be rewritten for antiferromagnets as

$$\hat{S}_j^z \rightarrow -\hat{S}_j^z \tag{13.68}$$

and

$$\hat{S}_j^{\pm} \rightarrow \hat{S}_j^{\mp}. \tag{13.69}$$

The Hamiltonian in Eq. (13.51) for ferromagnets can be rewritten for antiferromagnets as (Problem 13.11)

$$\hat{H} = 2|J| \sum_{<ij>} \left[-\hat{S}_{iz}\hat{S}_{jz} + \frac{1}{2}(\hat{S}_i^+ \hat{S}_j^+ + \hat{S}_i^- \hat{S}_j^-) \right], \tag{13.70}$$

where the factor of 2 is multiplied because each neighboring pair $<ij>$ appears twice in the summation over i and j. Using a procedure adapted to obtain Eq. (13.57) with the modifications for antiferromagnets (Eqs. 13.68 through 13.70), we obtain (Problem 13.12)

$$\begin{aligned} \hat{H} = 2|J| \sum_{<ij>} \Bigg[& -(S - \hat{a}_i^\dagger \hat{a}_i)(S - \hat{a}_j^\dagger \hat{a}_j) + \frac{1}{2}\hat{a}_i^\dagger \sqrt{2S - \hat{a}_i^\dagger \hat{a}_i}\, \hat{a}_j^\dagger \sqrt{2S - \hat{a}_j^\dagger \hat{a}_j} \\ & + \frac{1}{2}\sqrt{2S - \hat{a}_i^\dagger \hat{a}_i}\, \hat{a}_i \sqrt{2S - \hat{a}_j^\dagger \hat{a}_j}\, \hat{a}_j \Bigg]. \end{aligned} \tag{13.71}$$

We follow a $1/S$ expansion method similar to the procedure outlined in Eq. (13.57) and from Eqs. (13.70) and (13.71), we obtain (Problem 13.13)

$$\hat{H} = -|J|NzS^2 + 2|J|S \sum_{<i,j>} [\hat{a}_i^\dagger \hat{a}_i + \hat{a}_j^\dagger \hat{a}_j + \hat{a}_i^\dagger \hat{a}_j^\dagger + \hat{a}_i \hat{a}_j], \tag{13.72}$$

where N is the number of lattice sites, and z is the number of nearest neighbors of each site. We define the operators

$$\hat{a}_i = \frac{1}{\sqrt{N}} \sum_{\mathbf{k}} e^{i\mathbf{k}\cdot\mathbf{R}_i} \hat{b}_{\mathbf{k}} \tag{13.73}$$

and

$$\hat{a}_i^\dagger = \frac{1}{\sqrt{N}} \sum_{\mathbf{k}} e^{-i\mathbf{k}\cdot\mathbf{R}_i} \hat{b}_{\mathbf{k}}^\dagger. \tag{13.74}$$

Substituting Eqs. (13.73) and (13.74) in Eq. (13.72), we obtain (Problem 13.14)

$$\hat{H} = -|J|NzS^2 + |J|S|\sum_{\mathbf{k},l}[2\hat{b}_{\mathbf{k}}^\dagger \hat{b}_{\mathbf{k}} + (\hat{b}_{\mathbf{k}}^\dagger \hat{b}_{-\mathbf{k}}^\dagger + \hat{b}_{\mathbf{k}}\hat{b}_{-\mathbf{k}})\cos(\mathbf{k}\cdot\mathbf{R}_l)], \tag{13.75}$$

where $\mathbf{R}_l$ are nearest-neighbor vectors. To diagonalize the Hamiltonian, we introduce two new operators through the transformation,

$$\hat{b}_{\mathbf{k}} = (\sinh\beta_{\mathbf{k}})\hat{c}_{-\mathbf{k}}^\dagger + (\cosh\beta_{\mathbf{k}})\hat{c}_{\mathbf{k}}, \tag{13.76}$$

where β is real. Substituting Eq. (13.76), we can show that the Hamiltonian in Eq. (13.75) is diagonalized provided (Problem 13.14)

$$\tanh 2\beta_{\mathbf{k}} = -\frac{1}{z}\sum_l \cos(\mathbf{k}\cdot\mathbf{R}_l). \tag{13.77}$$

Substituting Eqs. (13.76) and (13.77) in Eq. (13.75), we obtain

$$\hat{H} = -N|J|zS(S+1) + 2|J|zS\sum_{\mathbf{k}}\left(\hat{b}_{\mathbf{k}}^\dagger \hat{b}_{\mathbf{k}} + \frac{1}{2}\right)\sqrt{1-\tanh^2 2\beta_{\mathbf{k}}}. \tag{13.78}$$

Thus, the ground-state energy is given by

$$\varepsilon_0 = -N|J|zS(S+1) + |J|zS\sum_{\mathbf{k}}\sqrt{1-\frac{1}{z^2}\left(\sum_l \cos\mathbf{k}\cdot\mathbf{R}_l\right)^2}, \tag{13.79}$$

and the energy of a magnon of wave number $\mathbf{k}$ is given by

$$\varepsilon_{\mathbf{k}} = 2|J|zS\sqrt{1-\frac{1}{z^2}\left(\sum_l \cos\mathbf{k}\cdot\mathbf{R}_l\right)^2}. \tag{13.80}$$

13.4 FERROMAGNETISM IN SOLIDS

13.4.1 Ferromagnetism Near the Curie Temperature

The spontaneous magnetization of a ferromagnet vanishes above the Curie temperature. This phenomenon can be explained by the exchange interaction by using the molecular field approximation. The Hamiltonian for the exchange interaction in the presence of an external field is given by

$$\hat{H} = -\sum_{ij}{}' J_{ij}\hat{\mathbf{S}}_i \cdot \hat{\mathbf{S}}_j - g\mu_B \mathbf{B}\cdot\sum_{i=1}^{N}\hat{\mathbf{S}}_i. \tag{13.81}$$

In the mean-field approximation, of which the validity is in general questionable, one of the operators appearing in the exchange integral is replaced by the mean value, so we can rewrite Eq. (13.81) as

$$\hat{H} = -\sum_{i=1}^{N}(g\mu_B \mathbf{B} + \sum_{j=1, j\neq i}^{N} J_{ij} <\hat{S}_j>) \cdot \hat{S}_i, \tag{13.82}$$

which we can rewrite in the alternate form

$$\hat{H} = -\sum_{i=1}^{N} g\mu_B(\mathbf{B} + \mathbf{B_M}). \tag{13.83}$$

Here, $\mathbf{B_M}$ is equivalent to the internal field originally introduced by Weiss to explain ferromagnetism. Assuming nearest-neighbor interaction between the spins, we obtain from Eqs. (13.82) and (13.83)

$$\mathbf{B_M} = \frac{zJ}{g\mu_B} <\hat{S}_j>. \tag{13.84}$$

If we further assume that $<\hat{S}_j>$ is in the same direction as the magnetization $\mathbf{M}$,

$$\mathbf{M} = Ng\mu_B <\hat{S}_j> \tag{13.85}$$

and

$$\mathbf{B_M} = \lambda \mathbf{M}, \tag{13.86}$$

where λ is the constant originally introduced by Weiss, known as the Weiss constant. From Eqs. (13.84) through (13.86), the relation between the Weiss constant λ and the exchange integral J is given by

$$\lambda = \frac{zJ}{Ng^2\mu_B^2}. \tag{13.87}$$

We obtain an expression for the spontaneous magnetic moment $\mathbf{M}$ for ferromagnetic solids ($\mathbf{B} = 0$) by following a procedure similar to that used earlier for the derivation of M for paramagnetic solids in Eq. (12.45),

$$M = NgS\mu_B B_s\left(\frac{g\mu_B S\lambda M}{k_B T}\right), \tag{13.88}$$

where the Brillouin function $B_s(x)$ was defined in Eq. (12.46),

$$B_S(x) = \frac{(2S+1)}{2S}\coth\left(\frac{2S+1}{2S}x\right) - \frac{1}{2S}\coth\frac{x}{2S}. \tag{13.89}$$

We note that for ferromagnetic solids, J is replaced with S in Eqs. (12.45) and (12.46). In addition, the external field $\mathbf{B} = 0$. We can easily check the accuracy of Eq. (13.89) by noting that when $T = 0$, coth $x = 1$ and $B_S = 1$. From Eqs. (13.88) and (13.89), we obtain the expression for saturation magnetization,

$$M = Ng\mu_B S. \tag{13.90}$$

When the temperature increases, the spins become randomly oriented, and the spontaneous magnetization gradually decreases until it disappears. The critical temperature T_C at which the spontaneous magnetization disappears is obtained from the following approximation for the Brillouin function $B_S(x)$. When $x \to 0$, which occurs when $M \to 0$,

$$B_S(x) \approx \frac{S+1}{S}\frac{x}{3} - \frac{(2S+1)^4 - 1}{(2S)^4}\frac{x^3}{45}. \tag{13.91}$$

Substituting Eq. (13.91) in (13.88), we obtain $(T \to T_C)$,

$$M \approx Ng^2\mu_B^2 S(S+1)\lambda M/3k_B T_C, \tag{13.92}$$

from which we obtain the expression for the critical temperature, known as the Curie temperature,

$$T_C = \frac{Ng^2\mu_B^2 S(S+1)\lambda}{3k_B}. \tag{13.93}$$

In the paramagnetic phase, the temperature dependence of magnetization can be described by the Curie law, provided the internal field is included along with the external field,

$$\mathbf{M} = \frac{C}{T}(\mathbf{B} + \lambda\mathbf{M}) \tag{13.94}$$

or

$$\mathbf{M} = \frac{C}{T - \lambda C}\mathbf{B}. \tag{13.95}$$

Further, we can write

$$\mathbf{M} = \chi\mathbf{B} = \frac{C}{T - T_C}\mathbf{B}, \tag{13.96}$$

from which we obtain the expression for the paramagnetic susceptibility χ,

$$\chi = \frac{C}{T - T_C}, \tag{13.97}$$

where T_C is the Curie temperature. From Eqs. (13.95) and (13.96), the Curie constant to be inserted in Eq. (13.97) is given by

$$C = \frac{T_C}{\lambda}, \tag{13.98}$$

where an expression for T_C was obtained in Eq. (13.93).

13.4.2 Comparison of Spin-Wave Theory with the Weiss Field Model

Both the spin-wave theory and the Weiss field model use the concept of direct exchange interaction between localized spins of nearest neighbors. The basic assumption in both models is that the electrons of a lattice ion contributing to the magnetic moment are tightly bound for the ions to be isolated, but the

nearest neighbors are sufficiently close for a significant interaction to arise. However, the results obtained by using the two models differ significantly at low and high temperatures. For example, from Eqs. (13.88) and (13.93), it can be easily shown that (Problem 13.15)

$$\frac{M(T)}{M(0)} = 1 - \frac{1}{S} e^{-3T_C/(S+1)T}, \tag{13.99}$$

while the experimental results agree with the $T^{3/2}$ law obtained by using spin-wave theory.

This result suggests that for temperatures near the ground state ($T = 0$), the spin-wave theory can be derived by using the method of elementary excitations rather than using other approximations. At higher temperatures, it is more appropriate to use semiclassical methods such as the Weiss field model, which can be justified by the general exchange-interaction concept. However, many aspects of the behavior of a ferromagnet near the Curie temperature can be understood by using the concept of magnons. Even at temperatures above the Curie temperature, paramagnons can be used to understand the properties in the paramagnetic region. The temperature dependence of the spontaneous magnetization, obtained from Eq. (13.88), is shown in Figure 13.5.

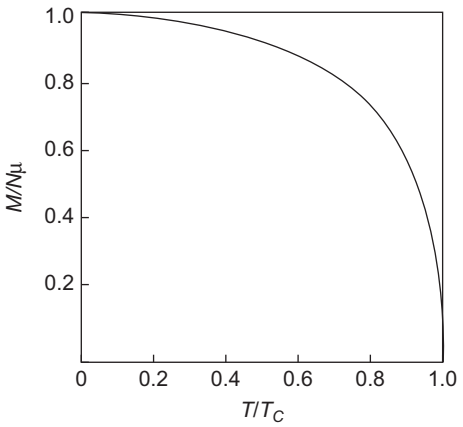

FIGURE 13.5
Saturation magnetization as a function of temperature.

13.4.3 Ferromagnetic Domains

It is a common experience to note that a ferromagnetic material is not necessarily magnetized when the temperature is lower than the Curie temperature. However, it is strongly attracted by magnetic fields and can be "magnetized" by stroking it with a "permanent magnet." The basic question is how the atomic magnetic dipoles are aligned below the Curie temperature and yet produce zero magnetization.

The key to explain this phenomenon is the fact that we have only considered the Heisenberg Hamiltonian while deriving an expression for the magnetization and neglected the magnetic dipolar interaction between the spins introduced in Eq. (13.7). The main reason for omitting the latter is that the dipolar coupling between nearest neighbors is much smaller than the exchange coupling. However, the exchange interaction is very short-ranged and decreases exponentially with spin separation in a ferromagnetic insulator. In contrast, the dipolar interaction falls off as the inverse cube of the separation. The magnetic configuration of a macroscopic sample depends on both interactions, especially when a large number of spins is involved where the dipolar energies that have been hitherto neglected become quite significant.

It can be easily shown that the dipolar energy can be substantially reduced by dividing the ferromagnetic solid into uniformly magnetized domains of much smaller size and of which the magnetization vectors point in different directions. The concept of ferromagnetic domains was introduced by Weiss. Figure 13.6 shows a schematic diagram of the domains in a ferromagnet (Ref. 7). The atomic dipoles are aligned in the same direction within a domain but have no common link with the neighboring domains.

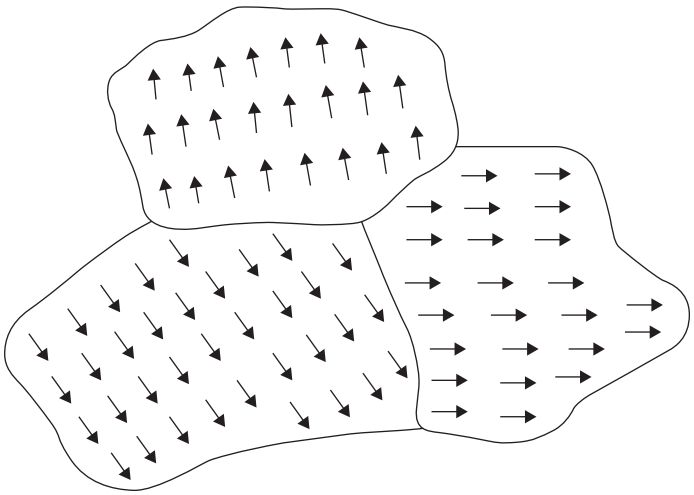

FIGURE 13.6

Ferromagnetic domains. The dimensions are 10 μm to 100 μm.

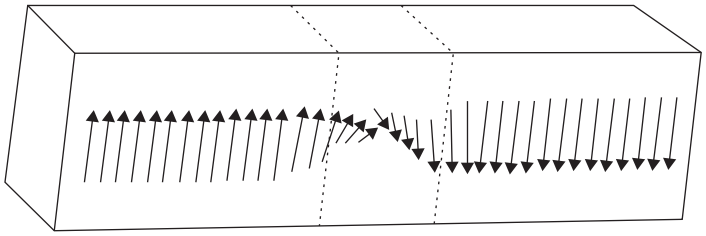

FIGURE 13.7

Schematic diagram of the change in orientation of magnetic dipoles in neighboring domains.

Figure 13.7 shows schematically a change in orientation of magnetic dipoles, in which each dipole is slightly misaligned with the neighboring dipole. The change in the orientation of the dipoles from the direction of one domain to that of the neighboring domain takes place over a distance of a few hundred atomic spaces. This narrow region between the adjacent domains is called a Bloch wall.

13.4.4 Hysteresis

Figure 13.8 shows the magnetization curve that describes the process by which a ferromagnetic material can be converted from a nonmagnetic state to a ferromagnetic state with the application of a reasonably small magnetic field. This curve is known as the hysteresis curve (Ref. 27). The magnetization curve is plotted as B versus H, where H is the external magnetic field and the magnetic induction, $B = H + 4\pi M$. The external field H is applied to an initially unmagnetized sample until the magnetization reaches the saturation value.

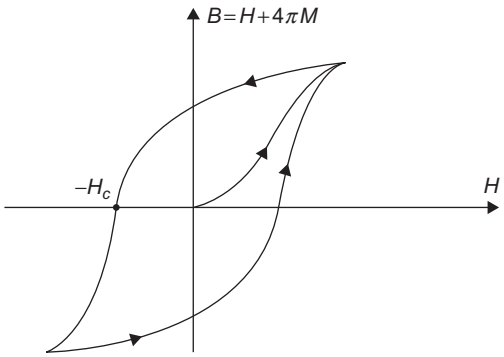

FIGURE 13.8

The hysteresis curve.

After the sample has become fully magnetized, the field is subsequently reduced, and the magnetization decreases to a constant value when the external field is zero. To return the sample to its original state (i.e., to demagnetize it), a magnetic field has to be applied in the opposite direction until $B = 0$ when $H = -H_c$. Usually, this is considered as the definition of the coercive force.

13.4.5 Ising Model

The Ising model is a very simplified version of the Heisenberg model. In this model, the Hamiltonian is written as

$$\hat{H} = -J\sum_{i,j}{}'\hat{S}_{iz}\hat{S}_{jz} - g\mu_B B\sum_{i=1}^{N}\hat{S}_{iz}. \tag{13.100}$$

Thus, the terms S^+ and S^- are essentially dropped from the Heisenberg model, and the magnetic field is taken in the z direction. Because all $\hat{S}_{iz}$ commute, the Hamiltonian $\hat{H}$ is diagonal in the representation in which each $\hat{S}_{iz}$ is diagonal. Hence, all the eigenfunctions and the eigenvalues of the Hamiltonian are known. Thus, the Ising model is very convenient in describing the statistical theory of phase transitions—for example, in describing the system when the ferromagnetic state is changed to a paramagnetic state at the Curie temperature. However, in spite of these simplifications, only by using a two-dimensional Ising model for simple lattices (i.e., square, triangular, honeycomb) can one calculate the exact free energy in zero magnetic field and the spontaneous magnetization. We will not discuss this model in more detail.

13.5 FERROMAGNETISM IN TRANSITION METALS

13.5.1 Introduction

The problem of the origin of ferromagnetism in some transition metals, of which the common feature is that they have narrow unfilled d-bands ($3d$) as well as filled s-bands (s^2), remains one of the major unsolved problems in solid state physics. There have been many theoretical explanations, but no theory can satisfactorily explain why Fe, Co, and Ni are ferromagnetic metals while a large number of transition elements with narrow unfilled d-bands are not ferromagnetic; i.e., they do not have spontaneous magnetization. For example, the configurations of these elements are

$$\mathrm{Fe}([\mathrm{Ar}]3d^6 4s^2), \quad \mathrm{Co}([\mathrm{Ar}]3d^7 4s^2), \quad \mathrm{Ni}([\mathrm{Ar}]3d^8 4s^2).$$

These three elements (Fe, Co, and Ni) are ferromagnetic metals, whereas Mn and Pd become ferromagnetic under certain conditions.

There have been many attempts to solve this problem of band ferromagnetism (Ref. 4). It is indeed easy to understand the origin of an atomic magnetic moment arising out of an intra-atomic

exchange but difficult to explain the cooperative interaction that couples the moments on different atoms. Such cooperative phenomena require a band model of ferromagnetism. However, one of the essential features of the band model is to delocalize the moment from the atom. Thus, the Heisenberg model is inappropriate for use in ferromagnetism in transition metals. We will discuss the existing theories, with the cautionary note that not one of them is adequate in explaining band ferromagnetism.

The magnetic moments of transition metals can indeed be calculated with reliable accuracy by using a combination of band calculations and density functional theory. However, this approach does not provide a specific model for band ferromagnetism.

13.5.2 Stoner Model

Stoner (Ref. 26) considered a collective electron model in which there is an interaction term between the pairs of electrons of opposite spin. Thus,

$$H_i = \frac{U}{N}\sum_{\mathbf{k},\mathbf{k}'} n_{\mathbf{k}\uparrow} n_{\mathbf{k}'\downarrow}, \tag{13.101}$$

where $n_{\mathbf{k}\uparrow(\downarrow)}$ is the occupation number of the states $|\mathbf{k}\uparrow(\downarrow)>\cdot$ Each pair of electrons of opposite spin contributes a positive "exchange" energy U/N. It should be made clear at this point that the nature of this positive "exchange" energy between opposite spins in the same d-shell was neither explained by Stoner nor has it been explained by any other group since then. In a later section, we will present an alternate interpretation for U. The contributions from electrons of the same spin in the d-shell are included in the definition of zero of energy and therefore not counted in Eq. (13.101). If we define the total number of electrons n_σ per atom of spin σ, the energy of an electron of $\uparrow(\downarrow)$ spin is

$$\varepsilon_{\mathbf{k}\uparrow(\downarrow)} = \varepsilon(\mathbf{k}) \mp \mu_B B + U n_{\downarrow(\uparrow)}. \tag{13.102}$$

The number of electrons in each state is given by two Fermi–Dirac distributions with the same chemical potential μ. Thus, we have

$$n_{\uparrow(\downarrow)} = \int_0^\infty D(\varepsilon) f^0(\varepsilon_{\mathbf{k}\uparrow(\downarrow)}) d\varepsilon, \tag{13.103}$$

where $f^0(\varepsilon_{\mathbf{k}\uparrow(\downarrow)})$ is the Fermi–Dirac distribution function, and $D(\varepsilon)$ is the density of states per spin. The chemical potential is the same for the two electron distributions. To satisfy this, the following conditions have to be met:

$$n<\mu> = \mu_B \int_0^\infty \{f^0(\varepsilon_{\mathbf{k}\uparrow}) - f^0(\varepsilon_{\mathbf{k}\downarrow})\} D(\varepsilon) d\varepsilon \tag{13.104}$$

and

$$n = \int_0^\infty \{f^0(\varepsilon_{\mathbf{k}\uparrow}) + f^0(\varepsilon_{\mathbf{k}\downarrow})\} D(\varepsilon) d\varepsilon. \tag{13.105}$$

The magnetic moment is given by

$$M = \mu_B (n_\uparrow - n_\downarrow). \tag{13.106}$$

From Eqs. (13.102), (13.103), and (13.106), we obtain

$$M = \mu_B \int_0^\infty \{f^0(\varepsilon - \mu_B B + Un_\downarrow) - f^0(\varepsilon + \mu_B B + Un_\uparrow)\} d\varepsilon, \tag{13.107}$$

which can be written in the alternate form in the limit of $B \to 0, T \to 0$,

$$M \approx [MU + 2\mu_B^2 B] \int_0^\infty \left(-\frac{\partial f^0}{\partial \varepsilon} D(\varepsilon) d\varepsilon \right). \tag{13.108}$$

At $T \to 0$, we have, for any function $F(\varepsilon)$,

$$-\int_0^\infty \frac{\partial f^0}{\partial \varepsilon} F(\varepsilon) d\varepsilon = F(\varepsilon_F). \tag{13.109}$$

From Eqs. (13.108) and (13.109), we obtain

$$M \approx [(MU + 2\mu_B^2 B) D(\varepsilon_F)]. \tag{13.110}$$

Eq. (13.110) can be rewritten in the alternate form

$$M \approx \frac{2\mu_B^2 B D(\varepsilon_F)}{1 - UD(\varepsilon_F)}. \tag{13.111}$$

The magnetic susceptibility is easily obtained from Eq. (13.111),

$$\chi = \frac{M}{B} = \frac{2\mu_B^2 D(\varepsilon_F)}{1 - UD(\varepsilon_F)}. \tag{13.112}$$

When the "exchange field" is sufficiently large so that

$$UD(\varepsilon_F) > 1, \tag{13.113}$$

Eq. (13.112) is unstable. In the Stoner model, this leads to a transition to ferromagnetism. In addition, from Eq. (13.106), to have a permanent magnetic moment,

$$n_\uparrow \gg n_\downarrow. \tag{13.114}$$

However, Stoner's model does not explain this large difference between $n_\uparrow$ and $n_\downarrow$. In addition, Stoner's model neither explains the origin of the positive "exchange interaction" U nor does it explain why only Fe, Co, and Ni are ferromagnetic metals among such a large number of elements in the transition group with narrow d-bands.

The typical density of states of iron and the other transition metals in the same group with $3d$ narrow bands and $4s$ wide bands is shown in Figure 13.9. Because the Fermi energy lies inside the $3d$ band, the density of states at the Fermi energy is very high.

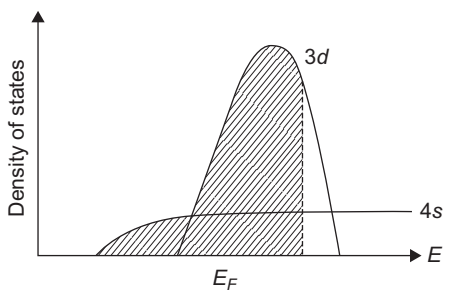

FIGURE 13.9

Schematic diagram of density of states of $3d$ and $4s$ bands in iron and other transition metals.

13.5.3 Ferromagnetism in Fe, Co, and Ni from Stoner's Model and Kohn–Sham Equations

In the 3*d* electrons in bulk transition metals, there is a significant overlap between neighboring atoms. The 4*s* electrons form broad free-electron-like bands of width 20–30 eV, whereas the 3*d* electron bandwidths are typically 5–10 eV. Due to hybridization and crystal environment, one electron is transferred from *s*- to *d*-bands. Thus, there are 7, 8, and 9 electrons per atom, respectively, in the *d*-bands in Fe, Co, and Ni. The predicted spin moments from Hund's rule are $\mu_{spin}(\text{Fe}) = 3\,\mu_B$, $\mu_{spin}(\text{Co}) = 2\,\mu_B$, and $\mu_{spin}(\text{Ni}) = \mu_B$. However, the actual values are noninteger and smaller because of partial delocalization; i.e., $\mu_{spin}(\text{Fe}) = 2.12\ \mu_B$, $\mu_{spin}(\text{Co}) = 1.58\,\mu_B$, and $\mu_{spin}(\text{Ni}) = 0.56\,\mu_B$.

Due to the large density of states, there are many unoccupied states just above the Fermi energy, which allows the promotion of electrons from minority spin to majority spin states at a modest energy cost. We have obtained the Stoner criterion for ferromagnetic susceptibility,

$$UD(\varepsilon_F) > 1. \tag{13.115}$$

The parameter U can be evaluated by perturbation theory based on non-spin-polarized solutions of the Kohn–Sham equations of density functional theory described in detail in Section 7.8.

Janak[9] showed that for infinitesimal Stoner splitting, one can write

$$U = \int d\mathbf{r}\, \gamma^2(\mathbf{r}) | K(\mathbf{r}), \tag{13.116}$$

where $\gamma(\mathbf{r})$ is essentially a normalized local density of states at the Fermi energy,

$$\gamma(\mathbf{r}) = \sum_i \frac{\delta(\varepsilon_F - \varepsilon_i)|\psi_i(\mathbf{r})|^2}{D(\varepsilon_F)}, \tag{13.117}$$

and ε_i and $\psi_i(\mathbf{r})$ are the self-consistent energies and wave functions of the Kohn–Sham equations. $K(\mathbf{r})$ is a kernel giving the exchange-correlation enhancement of the field due to magnetization defined by

$$\left\{ \frac{\delta^2 E_{xc}[nm]}{\delta m(\mathbf{r}) \delta m(\mathbf{r}')} \right\}_{m=0} = 2K(\mathbf{r})\delta(\mathbf{r} - \mathbf{r}'), \tag{13.118}$$

where $E_{xc}[n;m]$ is the exchange-correlation functional, which is defined in Eq. (7.165) in the local density approximation of Kohn and Sham. Here, n and m are defined in the usual manner,

$$n_\rho(\mathbf{r}) = \sum_i \theta(\varepsilon_F - \varepsilon_{i\rho})|\psi_{i\rho}|^2, \tag{13.119}$$

$$n(\mathbf{r}) = n_\uparrow(\mathbf{r}) + n_\downarrow(\mathbf{r}), \tag{13.120}$$

and

$$m(\mathbf{r}) = n_\uparrow(\mathbf{r}) - n_\downarrow(\mathbf{r}). \tag{13.121}$$

Janak (Ref. 9) calculated the values of both U and $D(\varepsilon_F)$ as functions of atomic number Z. The exchange-correlation-enhanced spin susceptibilities of 32 elements from Li through In were calculated using the spin-polarized exchange-correlation functional of von Barth and Hedin. The methods of Janak's calculation are summarized in his paper, and the results are tabulated in Table 1 of the same

paper [note that his results for $D(\varepsilon_f)$ are for both spins]. He has also plotted U and $D(\varepsilon_F)$ as a function of atomic number Z in Figure 13.1 of his paper. In Figure 13.10, we have plotted $1 - UD(\varepsilon_F)$ versus Z, where $D(\varepsilon_F)$ is the density of states per spin. We note that according to the data, both Fe (Z = 26) and Ni (Z = 28) are ferromagnetic according to the Stoner criterion while $UD(\varepsilon_F) = 0.97$ for Co (Z = 27). In contrast, calculations by Gunnarson (Ref. 4) indicate that $UD(\varepsilon_F)$ is in the range 1.6–1.8 for Co.

To summarize, the ferromagnetism of Fe, Co, and Ni can be explained by using density-functional theory through a combination of band theory and Stoner criterion, but we still lack a fundamental theory of ferromagnetism in transition metals.

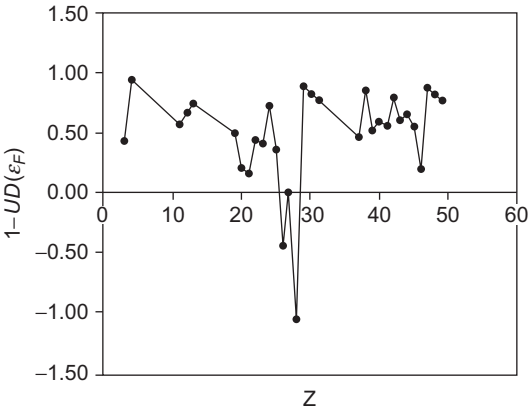

FIGURE 13.10

Using data from Figure 1 of Janak (Ref. 9), $1 - UD(\varepsilon_F)$ is plotted against Z (by Binns C and Blackman JA, p.231 of Ref. 19.).

Reproduced from Misra[19] with permission of Elsevier.

13.5.4 Free Electron Gas Model

It is well known that the free electron gas model does not explain the ferromagnetism in metals. However, one can derive conditions for the onset of ferromagnetism using the free electron gas model without using spin-dependent interactions. The free electron gas model provides a simple theory that is grossly inadequate but nevertheless provides a glimpse into the much harder and yet unsolved problem. It deals with the itinerant aspect of exchange through the use of the Hartree–Fock approximation of the uniform electron gas.

We derived in Eq. (7.44) an expression for the ground-state energy of the free electrons,

$$E = N\frac{e^2}{2a_0}\left[\frac{3}{5}(k_F a_0)^2 - \frac{3}{2\pi}(k_F a_0)\right], \tag{13.122}$$

where a_0 is the Bohr radius, the first term is the total kinetic energy, and the second term is the exchange energy that is between the electrons of the same spin.

Eq. (13.122) was derived with the assumption that each occupied one-electron state was occupied with two electrons of opposite spin. However, if it so happens that there is a spin imbalance, then each one-electron state has k less than some $k_\uparrow$ with spin-up electrons and similarly $k < k_\downarrow$ for some spin-down electrons. Because the exchange interaction is between electrons of the same spin, we obtain from Eq. (13.122) an equation for each spin population,

$$E_{(\uparrow,\downarrow)} = N_{(\uparrow,\downarrow)}\frac{e^2}{2a_0}\left[\frac{3}{5}(k_{(\uparrow,\downarrow)}a_0)^2 - \frac{3}{2\pi}(k_{(\uparrow,\downarrow)}a_0)\right]. \tag{13.123}$$

The total energy

$$E = E_\uparrow + E_\downarrow, \tag{13.124}$$

and the total number of electrons

$$N = N_\uparrow + N_\downarrow = V\left(\frac{k_\uparrow^3 + k_\downarrow^3}{6\pi^2}\right) = V\frac{k_F^3}{3\pi^2}. \tag{13.125}$$

If $N_\uparrow > N_\downarrow$, the ground state will have a nonvanishing magnetic density

$$M = -g\mu_B\frac{N_\uparrow - N_\downarrow}{V}, \tag{13.126}$$

which leads to a ferromagnetic electron gas. In the other extreme, if

$$\begin{aligned} N_\downarrow &= N, \\ N_\uparrow &= 0, \\ E &= E_\downarrow, \\ k_\downarrow &= 2^{1/3}k_F \text{ (from Eq. 13.125)}. \end{aligned} \tag{13.127}$$

From Eqs. (13.124), (13.125), and (13.127), we obtain

$$E_\downarrow = N\left[\frac{3}{5}2^{2/3}(k_F a_0)^2 - \frac{3}{2\pi}2^{1/3}(k_F a_0)\right]. \tag{13.128}$$

Comparing Eqs. (13.122) with (13.128), we note that the energy of the fully magnetized state is lower than the energy of the unmagnetized state when the exchange energy dominates the kinetic energy. It can be shown from Eq. (13.128) that when $E = E_\downarrow$, transition to a fully magnetized state occurs, in which case

$$k_F a_0 = \frac{5}{2\pi}\frac{1}{2^{1/3}+1}. \tag{13.129}$$

We earlier defined the electron density r_s,

$$r_s = \left(\frac{3V}{4\pi N}\right)^{1/3} = \frac{1.92}{k_F}. \tag{13.130}$$

From Eqs. (13.129) and (13.130), the condition for transition from a nonmagnetic to a ferromagnetic state is

$$\frac{r_s}{a_0} = \frac{2\pi}{5}(2^{1/3}+1)\left(\frac{9\pi}{4}\right)^{1/3} = 5.45. \tag{13.131}$$

The only metal with such a low conduction electron density is cesium. There are some metallic compounds that also satisfy the criteria that $r_s/a_0 > 5.45$.

However, none of these are ferromagnetic metals, even though their band structures are reasonably described by the free electron model. Thus, one has to know the specific features of the band structure and the itinerant exchange interactions to be able to account for magnetic ordering. The starting point is the fact that the *d*-electrons form a narrow band. Next, we will briefly discuss a few models for the theory of ferromagnetic metals.

13.5.5 Hubbard Model

Hubbard (Ref. 8) proposed a simple model that yields both bandlike and localized behavior in suitable limits. He proposed an extension of the tight-binding model by adding a term that includes an energy penalty U for any atomic site occupied by more than one electron. Hubbard's main argument was that because the off-diagonal elements of the Coulomb interaction were much smaller than the diagonal elements, the Hamiltonian can be approximated as

$$\hat{H} = \sum_{<ij>,\rho} -t[\hat{a}^{\dagger}_{i\rho}\hat{a}_{j\rho} + \hat{a}^{\dagger}_{j\rho}\hat{a}_{i\rho}] + U\sum_{i} \hat{a}^{\dagger}_{i\uparrow}\hat{a}_{i\uparrow}\hat{a}^{\dagger}_{i\downarrow}\hat{a}_{i\downarrow}, \tag{13.132}$$

where the sum $<ij>$ is taken over nearest-neighbor pairs. Here, the off-diagonal states have nonvanishing matrix elements t, known as the hopping parameter, between those pairs of states that differ only by a single electron that has moved from an ion to one of its neighbors without change of spin. This set of terms leads to a tight-binding model of one-electron Bloch levels. Even this oversimplified Hamiltonian can be solved only by using mean-field theory.

Eq. (13.132) can be rewritten as

$$\hat{H} = \sum_{<ij>,\rho} -t[\hat{a}^{\dagger}_{i\rho}\hat{a}_{j\rho} + \hat{a}^{\dagger}_{j\rho}\hat{a}_{i\rho}] + U\sum_{i} \hat{n}_{i\uparrow}\hat{n}_{i\downarrow}. \tag{13.133}$$

If we write

$$\hat{n}_{i\rho} = n_{\rho} + (\hat{n}_{i\rho} - n_{\rho}), \tag{13.134}$$

and consider the second term in Eq. (13.134) as small, Eq. (13.133) can be rewritten as

$$\hat{H} = \sum_{<ij>,\rho} -t[\hat{a}^{\dagger}_{i\rho}\hat{a}_{j\rho} + \hat{a}^{\dagger}_{j\rho}\hat{a}_{i\rho}] + U\sum_{i} (\hat{n}_{i\uparrow}n_{\downarrow} + n_{\uparrow}\hat{n}_{i\downarrow} - n_{\uparrow}n_{\downarrow}). \tag{13.135}$$

Making a Fourier transformation of the type

$$\hat{a}_{i\rho} = \frac{1}{\sqrt{N}} \sum_{\mathbf{k}} e^{i\mathbf{k}\cdot\mathbf{R}_i} \hat{b}_{\mathbf{k}\rho}, \tag{13.136}$$

from Eqs. (13.135) and (13.136), we obtain (Problem 13.17)

$$\hat{H} = \sum_{\mathbf{k},\mathbf{R}_l,\rho} -t\hat{b}^{\dagger}_{\mathbf{k}\rho}\hat{b}_{\mathbf{k}\rho} \cos \mathbf{R}_l \cdot \mathbf{k} + U\sum_{\mathbf{k}} (\hat{n}_{\mathbf{k}\uparrow}n_{\downarrow} + n_{\uparrow}\hat{n}_{\mathbf{k}\downarrow} - n_{\uparrow}n_{\downarrow}), \tag{13.137}$$

where $\mathbf{R}_l$ are nearest-neighbor vectors. The Hamiltonian in Eq. (13.137) becomes diagonal in $\mathbf{k}$ space. Specific calculations for a ferromagnetic solid (Ref. 30) can be made depending on the lattice structure and the dimension. In addition to the difficulties in making specific calculations in the Hubbard model, its major drawback is that it was designed for solutions that lead to ferromagnetism in metals.

We will present an alternate model for ferromagnetism in the transition metals starting with a theory of magnetization of interacting Bloch electrons.

13.6 MAGNETIZATION OF INTERACTING BLOCH ELECTRONS

13.6.1 Introduction

Recently, Tripathi and Misra[29] derived a theory of magnetization of interacting electrons in the presence of a periodic potential, spin-orbit interaction, and an applied magnetic field in the paramagnetic limits. Starting from a thermodynamic potential, which includes both the quasiparticle and correlation contributions, they showed that the modifications brought about by the electron–electron interactions for the magnetization in the quasiparticle approximation are precisely canceled by the contributions due to electron correlations. The magnetization is expressed as a product of the spin density and effective g factor, due mainly to the spin-orbit interaction. Tripathi and Misra (Ref. 29) also showed the importance of the self-energy corrections in the single-particle energy spectrum. By considering a variant of the Hubbard Hamiltonian in the momentum space, their theory can predict whether or not the ground state of the interacting electron system is magnetic. Tripathi and Misra's model for ferromagnetism appears as a variant of the Stoner model but from a very different perspective.

13.6.2 Theory of Magnetization

The magnetization of an interacting electron system is given by

$$M^{v} = -\frac{\partial \Omega}{\partial B^{v}}, \tag{13.138}$$

where Ω is the thermodynamic potential, and in Eq. (12.123), Misra et al. (Ref. 18) showed

$$\Omega = \Omega_{qp} + \Omega_{corr}, \tag{13.139}$$

where

$$\Omega_{qp} = \frac{1}{\beta} Tr\, \ln(-\widetilde{G}_{\xi_l}) = -\frac{1}{2i\pi} Tr \oint_C F(\xi)\widetilde{G}(\xi)d\xi, \tag{13.140}$$

$$F(\xi) = -\frac{1}{\beta} \ln\left[1 + e^{-\beta(\xi-\mu)}\right], \tag{13.141}$$

and the contour encircles the imaginary axis in a counterclockwise direction and Tr involves summation over one-particle states.[18] Misra et al.[18] derived (Eq. 12.117)

$$[\xi_l - \hat{H}(\overrightarrow{\kappa}, \xi_l)]\hat{G}(\mathbf{k}, \xi_l) = I, \tag{13.142a}$$

where

$$\overrightarrow{\kappa} = \mathbf{k} + i\mathbf{h} \times \nabla_{\mathbf{k}}, \tag{13.142b}$$

(from Eq. 12.119) and $\mathbf{h} = \frac{e\mathbf{B}}{2\hbar c}$ (from Eq. 12.114).

Misra et al. (Ref. 18) also derived (Eqs. 12.130 through 12.132)

$$\hat{H}(\overrightarrow{\kappa}, \xi_l) = \hat{H}_0(\mathbf{k}, \xi_l) + \hat{H}'(\mathbf{k}, \xi_l), \tag{13.143}$$

where

$$\hat{H}_0(\mathbf{k},\xi_l) = \frac{1}{2m}(\mathbf{p}+\hbar\mathbf{k})^2 + V(\mathbf{r}) + \Sigma^0(\mathbf{k},\xi_l) + \frac{\hbar^2}{8mc^2}\nabla^2 V + \frac{\hbar}{4m^2c^2}\overrightarrow{\sigma}\cdot\overrightarrow{\nabla}V\times(\mathbf{p}+\hbar\mathbf{k}), \tag{13.144}$$

and retaining terms up to the first order in the magnetic field in Eq. (12.132),

$$H'(\mathbf{k},\xi_l) = -ih_{\alpha\beta}\Pi^\alpha\nabla^\beta_{\mathbf{k}} + \tfrac{1}{2}g\mu_B B^\mu\sigma^\mu + B^\mu\Sigma^{1,\mu}(\mathbf{k},\xi_l). \tag{13.145}$$

In Eq. (13.145), $h_{\alpha\beta} = \in_{\alpha\beta\mu} h^\mu$, where $\in_{\alpha\beta\mu} h^\mu$, where $\in_{\alpha\beta\mu}$ is the antisymmetric tensor of the third rank and we follow Einstein summation convention.

Here, $\overrightarrow{\Pi}$ was defined in Eq. (12.133),

$$\overrightarrow{\Pi} = \frac{\hbar}{m}(\mathbf{p}+\hbar\mathbf{k}) + \frac{\hbar^2}{4m^2c^2}\overrightarrow{\sigma}\times\overrightarrow{\nabla}V + \nabla_{\mathbf{k}}\Sigma^0(\mathbf{k},\xi_l). \tag{13.146}$$

In addition, from Eqs. (12.134) through (12.136), Misra et al. (Ref. 18) derived

$$\widetilde{G}(\mathbf{k},\xi_l) = G_0(\mathbf{k},\xi_l) + G_0(\mathbf{k},\xi_l)\hat{H}'G_0(\mathbf{k},\xi_l) + \cdots \tag{13.147}$$

and

$$\nabla^\alpha_{\mathbf{k}}G_0(\mathbf{k},\xi_l) = G_0(\mathbf{k},\xi_l)\Pi^\alpha G_0(\mathbf{k},\xi_l), \tag{13.148a}$$

where (from Eq. 12.135)

$$G_0(\mathbf{k},\xi_l) = \frac{1}{\xi_l - \hat{H}_0(\mathbf{k},\xi_l)}. \tag{13.148b}$$

From Eqs. (13.145) through (13.148), it can be shown that (Problem 13.18)

$$\widetilde{G}(\mathbf{k},\xi_l) = G_0 - G_0\left[ih_{\alpha\beta}\Pi^\alpha\nabla^\beta_{\mathbf{k}} - \frac{1}{2}g\mu_B B^\nu F^\nu\right]G_0, \tag{13.149}$$

where

$$F^\nu = \sigma^\nu + \frac{2}{g\mu_B}\widetilde{\Sigma}^{1,\nu} \tag{13.150}$$

was defined in Eq. (12.147) and is the renormalized spin vertex in the presence of the electron–electron interaction.

13.6.3 The Quasiparticle Contribution to Magnetization

From Eqs. (12.123) and (13.149), one can obtain the quasiparticle contribution to the thermodynamic potential, after evaluating the trace and contour integration (Problem 13.19) as

$$\Omega_{qp} = \frac{1}{2}\mu_B B^\nu \sum_{n\mathbf{k}\rho m\rho',m\neq n}\left[gF^\nu_{n\rho,n\rho'} + \frac{ie}{\hbar c\mu_B}\in_{\alpha\beta\nu}\frac{\Pi^\alpha_{n\rho,m\rho'}\Pi^\beta_{m\rho',n\rho}}{E_{mn}}\right]f(E_{n\mathbf{k}\rho}), \tag{13.151}$$

where $f(E_{n\mathbf{k}\rho})$ is the Fermi distribution function for an electron in band n and spin ρ,

$$\Pi^\alpha_{n\rho,m\rho'} = \int_{cell} d^3r u^*_{n\mathbf{k}\rho}\Pi^\alpha u_{m\mathbf{k}\rho'} \tag{13.152}$$

and

$$E_{mn} = E_m(\mathbf{k}) - E_n(\mathbf{k}). \tag{13.153}$$

Using

$$M^v_{qp} = -\frac{\partial \Omega_{qp}}{\partial B^v}, \tag{13.154}$$

and Eqs. (13.150) and (13.151), Tripathi and Misra (Ref. 29) obtain

$$M^v_{qp} = -\frac{1}{2}\mu_B \sum_{n\mathbf{k}\rho\rho'} \left[g^v_{nn}(\mathbf{k})\sigma^v_{n\rho,n\rho'} + \frac{2}{\mu_B}\widetilde{\Sigma}^{1,v}_{n\rho,n\rho'} \right] f(E_{n\mathbf{k}\rho}), \tag{13.155}$$

where

$$g^v_{nn}(\mathbf{k})\sigma^v_{n\rho,n\rho'} = g\sigma^v_{n\rho,n\rho'} + \frac{ie}{\hbar c\mu_B} \in_{\alpha\beta v} \sum_{m\neq n,\rho'} \frac{\Pi^\alpha_{n\rho,m\rho'}\Pi^\beta_{mv',n\rho}}{E_{mn}}, \tag{13.156}$$

and is the effective g factor in the presence of spin-orbit interaction. In the absence of spin-orbit interactions, the second term in Eq. (13.156) vanishes, and the effective g factor reduces to the free electron g factor. In the absence of many-body interactions, the second term in the square brackets of Eq. (13.155) vanishes. However, Tripathi and Misra (Ref. 29) showed that the inclusion of M_{corr} would precisely cancel this term, and the final expression for magnetization would be free from any explicit many-body corrections—a surprising result that we will discuss in detail at the end of this section.

13.6.4 Contribution of Correlations to Magnetization

In Eq. (12.123), Misra et al. (Ref. 18) derived

$$\Omega_{corr} = \frac{1}{\beta}\left[-Tr\,\widetilde{\Sigma}_{\xi_l}\widetilde{G}_{\xi_l} + \phi(\widetilde{G}_{\xi_l}) \right]. \tag{13.157}$$

The contribution of correlation to magnetization is (Ref. 29)

$$M^v_{corr} = -\frac{\partial \Omega_{corr}}{\partial B^v} = \frac{1}{\beta} Tr\, \frac{\partial \widetilde{\Sigma}_{\xi_l}}{\partial B^v}\widetilde{G}_{\xi_l}. \tag{13.158}$$

Simplifying Eq. (13.158) with the use of Eqs. (12.127), (12.128), (13.155), and the Luttinger–Ward (Ref. 15) prescription for frequency summation, we obtain

$$\frac{1}{\beta}\sum_{\xi_l} \frac{1}{(\xi_l - \hat{H}_0)^m} = \frac{1}{2i\pi} Tr \int_{\Gamma_0} \frac{1}{(\xi - \hat{H}_0)^m} f(\xi) d\xi, \tag{13.159}$$

where Γ_0 encircles the real axis in a clockwise direction, and $f(\xi)$ is the Fermi distribution function obtained (Problem 13.20) after evaluating the *tr* over a complete set of single particle states,

$$M^v_{corr} = \sum_{n\mathbf{k}\rho} \widetilde{\Sigma}^{1,v}_{n\rho,n\rho'} f(E_{n\mathbf{k}\rho}) \cdot \tag{13.160}$$

From Eqs. (13.155) and (13.160),

$$M^v = -\frac{1}{2}\mu_B \sum_{n\mathbf{k}\rho\rho'} g^v_{nn}(\mathbf{k})\sigma^v_{n\rho,n\rho'} f(E_{n\mathbf{k}\rho}). \tag{13.161}$$

Thus, the renormalization of the spin vertex by the electron–electron interactions in the quasiparticle contribution is precisely canceled by M^v_{corr}. It may appear surprising that although both the spin contribution to the susceptibility (Ref. 18) (see Chapter 12) and spin Knight shift (Ref. 28) are exchange enhanced by electron–electron interactions, the self-energy corrections do not explicitly appear in the expression for magnetization. The reason is that the magnetic susceptibility and Knight shift arise from second-order effects in the magnetic field, where both the spin vertices are renormalized, and the renormalization of only one of the vertices is canceled due to the electron correlations. The renormalization of the other spin vertex, in a Hartree–Fock analysis, contributes to the exchange enhancement of the spin contributions to the susceptibility (Chapter 12) and Knight shift. In contrast, the single-particle energies appearing in Eqs. (13.144) and (13.145) depend on electron–electron interaction and the magnetic field through the self-energy. In the next section, we will show the consequences of these self-energy corrections on the single-particle spectrum in predicting whether or not the ground state of the interacting system is magnetic.

Assuming the effective magnetic field to be in the z direction and considering a single band, Tripathi and Misra (Ref. 29) obtained a tractable expression by averaging over the g matrix and denoting it as the effective g factor g_{eff}. They showed that Eq. (13.161) can be expressed as

$$M = -\frac{1}{2}\mu_B g_{eff} \sum_{\mathbf{k}\rho\rho'} \sigma_{\rho\rho'} f(E_{\mathbf{k}\rho}). \tag{13.162}$$

Here, ρ and ρ' take both $\uparrow$ and $\downarrow$ states. Eq. (13.162), therefore, can be rewritten as

$$M = -\frac{1}{2}\mu_B g_{eff}(n_\uparrow - n_\downarrow), \tag{13.163}$$

where

$$n_{\uparrow(\downarrow)} = \sum_{\mathbf{k}} f(E_{\mathbf{k}\uparrow(\downarrow)}). \tag{13.164}$$

13.6.5 Single-Particle Spectrum and the Criteria for Ferromagnetic Ground State

The single-particle energies $E_{\mathbf{k}\rho}$ appearing in Eq. (13.154) are the eigenvalues of the field-independent Hamiltonian described in Eq. (13.144). If the spin-orbit interaction is neglected, ρ becomes a pure spin state, and $E_{\mathbf{k}\rho}$ can be obtained by the following procedure. The many-body Hamiltonian can be written as

$$\hat{H}_0 = \sum_{\mathbf{k}\rho} \varepsilon_{\mathbf{k}} c^\dagger_{\mathbf{k}\rho} c_{\mathbf{k}\rho} + \frac{1}{2}\sum_{\mathbf{q}\mathbf{k}\mathbf{k}'\rho\rho'} V(\mathbf{q}) c^\dagger_{\mathbf{k}+\mathbf{q},\rho} c^\dagger_{\mathbf{k}'-\mathbf{q},\rho'} c_{\mathbf{k}',\rho'} c_{\mathbf{k},\rho}, \tag{13.165}$$

where $c^\dagger_{\mathbf{k}\rho}$ and $c_{\mathbf{k}\rho}$ are the creation and annihilation operators for an electron with wave vector $\mathbf{k}$ and spin ρ, and $V(\mathbf{q})$ is the Fourier transformation of the Coulomb interaction.

$E_{\mathbf{k}\rho}$ can be obtained by using the mean-field approximation,

$$E_{\mathbf{k}\rho} = \frac{1}{N}\left\langle \left\{ [c_{\mathbf{k}\rho}, \hat{H}_0], c^{\dagger}_{\mathbf{k}\rho} \right\} \right\rangle. \tag{13.166}$$

From Eqs. (13.165) and (13.166), we obtain

$$E_{\mathbf{k}\rho} = \varepsilon_{\mathbf{k}} - \frac{1}{N}\sum_{\mathbf{q}} V(\mathbf{q}) f(\varepsilon_{\mathbf{k}-\mathbf{q},\rho}) + \frac{1}{N} V(0) \sum_{\mathbf{k}} [f(\varepsilon_{\mathbf{k}\rho}) + f(\varepsilon_{\mathbf{k},-\rho})]. \tag{13.167}$$

Because V is assumed to be a constant U in the approximation of the averaged Coulomb interaction ansatz, we can rewrite Eq. (13.167) as

$$E_{\mathbf{k}\rho} = \varepsilon_{\mathbf{k}} + \frac{1}{N} U \sum_{\mathbf{k}} f(\varepsilon_{\mathbf{k},-\rho}) \equiv \varepsilon_{\mathbf{k}} + U n_{-\rho}, \tag{13.168}$$

where

$$n_{-\rho} = \frac{1}{N}\sum_{\mathbf{k}} f(\varepsilon_{\mathbf{k},-\rho}). \tag{13.169}$$

Eq. (13.168) is the Hartree–Fock representation of the single-particle spectrum. If we write $n = n_{\uparrow} + n_{\downarrow}$ and $m = n_{\uparrow} - n_{\downarrow}$ where n is the number of electrons/atoms and m is the average magnetization per atom in a Bohr magneton, the total energy per atom is

$$E = \frac{1}{N}\sum_{\mathbf{k}\rho} \varepsilon_{\mathbf{k}} f(E_{\mathbf{k}\rho}) + U n_{\uparrow} n_{\downarrow}. \tag{13.170}$$

The nonmagnetic solution in the ground state is obtained from the criteria

$$\begin{aligned} f(E_{\mathbf{k}\rho}) &= 1 \text{ if } E_{\mathbf{k}\rho} < E_F \\ &= 0 \text{ if } E_{\mathbf{k}\rho} > E_F. \end{aligned} \tag{13.171}$$

The Fermi energy E_F is determined from the condition that one has the right number (n) of electrons per atom. To study the stability of this state, let us transfer some electrons in an energy range δE below E_F from the down-spin states to the up-spin states. The change in the kinetic energy is

$$\Delta T = D(E_F)(\delta E^2), \tag{13.172}$$

where $D(E_F)$ is the density of states per atom per spin at the Fermi energy. The change in the interaction energy is

$$\Delta E_{int} = U\left(\frac{n}{2} + D\delta E\right)\left(\frac{n}{2} - D\delta E\right) - \frac{1}{4}Un^2 \equiv -UD^2(E_F)(\delta E^2). \tag{13.173}$$

From Eqs. (13.172) and (13.173), the change in the total energy is

$$\Delta E = D(E_F)(\delta E)^2[1 - UD(E_F)]. \tag{13.174}$$

The nonmagnetic state would be stable if $UD(\varepsilon_F) < 1$ and the condition for the ferromagnetic stability is $UD(\varepsilon_F) > 1$. This appears similar to the Stoner condition for ferromagnetic stability except that here U is well defined (Eq. 13.168) instead of an arbitrary positive attractive interaction between electrons of opposite spin in an atom. It can be shown that the preceding conditions could

also be obtained if one considers the second-order terms in the field in the thermodynamic potential and calculates the magnetic susceptibility.

13.7 THE KONDO EFFECT

In 1936, de Haas and van den Berg observed in experiments with gold (probably containing a small amount of iron impurities) that electrical resistivity dropped as the normal temperature decreased until about 8° K, and below that it increased. This observation was in contrast to the theory of electrical resistivity of normal metals (nonsuperconductors) where the resistance is supposed to fall with temperature as the atomic vibrations decrease and, below about 10° K, remain constant. This low-temperature residual resistivity is due to scattering by defects in the material.

Kondo (Ref. 14) used second-order perturbation theory to calculate the scattering of the conduction electrons of a noble metal by magnetic defects, using a Heisenberg model to describe the interaction between conduction electron spins and the spin moments and the defects. Kondo observed that spin-flip processes can occur in the second order, which results in a resistance that increases logarithmically when the temperature is lowered. These results are valid above a temperature T_K (known as the Kondo temperature), but the perturbation theory breaks down for $T < T_K$. In 1963, Nagaoka[20] published a self-consistent treatment that yielded solutions both above and below the Kondo temperature and reproduced the resistance minimum.

13.8 ANDERSON MODEL

In 1961, Anderson (Ref. 1) proposed a model for the Hamiltonian of a single magnetic impurity to a Fermi sea of electrons,

$$H = \sum_{\mathbf{k}\sigma} \varepsilon_{\mathbf{k}} c^{\dagger}_{\mathbf{k}\sigma} c_{\mathbf{k}\sigma} + \varepsilon_d \sum_{\sigma} d^{\dagger}_{\sigma} d_{\sigma} + \sum_{\mathbf{k}\sigma} (V_{d\mathbf{k}} d^{\dagger}_{\sigma} c_{\mathbf{k}\sigma} + V^{*}_{d\mathbf{k}} c^{\dagger}_{\mathbf{k}\sigma} d_{\sigma}) + U d^{\dagger}_{\uparrow} d_{\uparrow} d^{\dagger}_{\downarrow} d_{\downarrow}. \tag{13.175}$$

The first term is the kinetic energy of the electrons, where $c^{\dagger}_{\mathbf{k}\sigma}$ and $c_{\mathbf{k}\sigma}$ are the creation and annihilation operators for electrons with spin σ in state $\mathbf{k}$. The magnetic state is represented by a single state with energy ε_d and electron operators $d^{\dagger}_{\sigma}$ and d_{σ}. The third term represents the $s-d$ hybridization of the d-level with the conduction band. The fourth term represents the cost, in Coulomb energy, of double occupancy of the d-level. U is assumed to be large and $\varepsilon < \varepsilon_F$, where ε_F is the Fermi energy. In the absence of the hybridization term, we have a single occupied (magnetic) d state. The Anderson model does not attempt to describe the details of the atomic $3d$ orbitals, but it captures the essential physics of the Kondo problem.

The Anderson Hamiltonian leads to the spin exchange process. The electron can tunnel from the localized impurity state to an unoccupied state just above the Fermi energy, and another electron from the Fermi energy sea replaces it. If these two electrons have opposite spin, it is known as a spin-flip process. An alternate spin-flip process involves double occupancy of the impurity state, with a cost of Coulomb energy. When many such processes are taken together, a new many-body process known as the Kondo resonance is generated. The Kondo resonance, which has a spin-singlet state, has a width of $k_B T_K$ and is pinned at the Fermi level, as schematically shown in Figure 13.11.

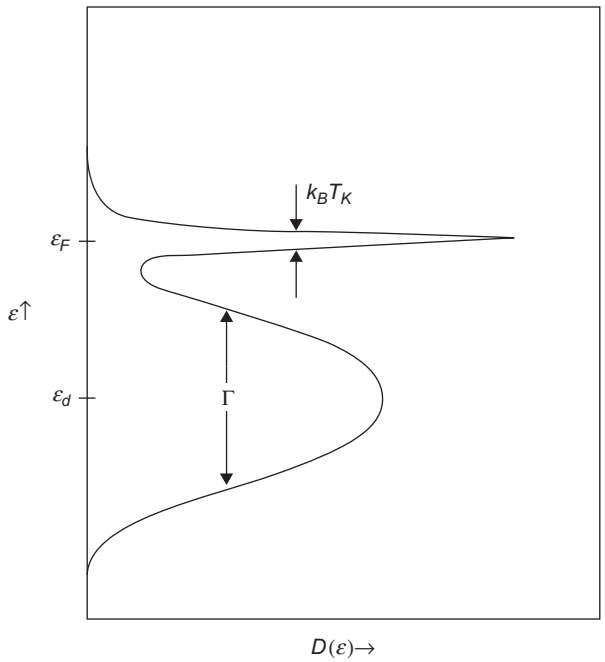

FIGURE 13.11

Schematic diagram of Kondo resonance of width $k_B T_K$. The impurity state is broadened to width Γ by hybridization with the conduction electrons.

The impurity state at ε_d is shifted and broadened through hybridization with electron states of the Fermi sea. This is known as a d-resonance. The net effect is an alignment of the spins of the conduction electrons near the impurity atom so that the local moment is screened. It has been shown by scaling laws and parameters of the Anderson model that

$$k_B T_K = \frac{1}{2}(\Gamma U)^{\frac{1}{2}} \exp\left[\pi \varepsilon_d (\varepsilon_d + U)/\Gamma U\right]. \tag{13.176}$$

13.9 THE MAGNETIC PHASE TRANSITION

13.9.1 Introduction

There are several types of phase transitions, but the most thoroughly investigated type is the paramagnetic to ferromagnetic phase transition. When the temperature is lowered through a critical temperature T_c of the system, a long-range order appears that was absent above T_c. The order, which usually has an infinite derivative at T_c, rapidly increases below T_c. In the absence of external fields, the ordering is not completely determined, and the transition is characterized by divergence of certain quantities like the magnetic susceptibility and the specific heat.

13.9.2 The Order Parameter

In the case of magnetization, the order parameter $\sigma(\mathbf{r})$, which describes the sudden appearance of order in the phase transition, is defined as

$$\sigma(\mathbf{r}) = M_z/M_0, \tag{13.177}$$

where M_z is the magnetization that defines the z-axis, and M_0 is the maximum possible value of magnetization,

$$M_0 = Ng\beta S. \tag{13.178}$$

The order parameter, which is zero above but not below T_c, can continuously approach zero as $T \to T_c$ from below if the transition is not of the first order. However, it is not completely determined below T_c in the absence of external fields.

13.9.3 Landau Theory of Second-Order Phase Transitions

According to Landau theory (Ref.15), the free energy is defined as a function of the order parameter

$$G = G(T, \sigma) = \int g(\mathbf{r}) d\mathbf{r}, \tag{13.179}$$

where $g(\mathbf{r})$ is the free energy density. The entropy S is given by

$$S = -\left(\frac{\partial G}{\partial T}\right)_\sigma. \tag{13.180}$$

Landau introduced a quantity $h(\mathbf{r})$, which is related to the external field $H_0(\mathbf{r})$ by

$$h(\mathbf{r}) = M_0 H(\mathbf{r}). \tag{13.181}$$

Landau assumed that $g(\mathbf{r})$ can be expanded as a power series in σ,

$$g(\mathbf{r}) = g_0(T) - h(\mathbf{r})\sigma(\mathbf{r}) + \alpha(T)[\sigma(\mathbf{r})]^2 + \beta(T)[\sigma(\mathbf{r})]^4 + \gamma(T)|\nabla\sigma(\mathbf{r})|^2 + \cdots. \tag{13.182}$$

Here, g is minimized (which determines the most probable value of σ) by requiring that

$$\delta \int g(\mathbf{r}) d\mathbf{r} = 0, \tag{13.183}$$

from which we obtain

$$\int d\sigma[-h(\mathbf{r}) + 2a\sigma + 4b\sigma^3 - 2c\,\nabla^2\sigma(\mathbf{r})] d\mathbf{r} = 0. \tag{13.184}$$

Eq. (13.184) yields

$$-2c\nabla^2\sigma(\mathbf{r}) + [2a + 4b\sigma^2(\mathbf{r})]\sigma(\mathbf{r}) = h(\mathbf{r}). \tag{13.185}$$

If σ and h are assumed to be independent of $\mathbf{r}$, Eq. (13.185) yields

$$[2a + 4b\sigma^2]\sigma = h. \tag{13.186}$$

If $h = 0$, the two possible solutions are

$$\sigma = 0 \tag{13.187}$$

and

$$\sigma = \pm(-a/2b)^{1/2}. \tag{13.188}$$

From Eqs. (13.182) and (13.183), if $a > 0$, Eq. (13.187) minimizes the free energy, whereas if $a < 0$, Eq. (13.188) minimizes the free energy. The free energy should describe a system with non-zero magnetization in the absence of external fields for $T < T_c$. This suggests the assumption

$$a(T) = \alpha(T - T_c), \tag{13.189}$$

where α is a constant. From Eqs. (13.188) and (13.189), we obtain

$$\sigma(T) \approx (T_c - T)^{1/2}, \quad (T < T_c). \tag{13.190}$$

Eq. (13.190) is consistent with the molecular field theory. To obtain the reduced susceptibility, we consider $h \neq 0$. The reduced susceptibility is defined as

$$\chi_r = (\partial\sigma/\partial h)_T. \tag{13.191}$$

From Eq. (13.186) and (13.191), we obtain

$$2a\chi_r + 12\sigma^2\chi_r = 1. \tag{13.192}$$

Because σ^2 is small and, hence, can be neglected for $T > T_c$, Eq. (13.192) can be rewritten in the alternate form with the help of Eq. (13.189),

$$\chi_r = 1/2\alpha(T - T_c), \quad (T > T_c). \tag{13.193}$$

Eq. (13.193) is the Curie–Weiss law. Below T_c, from Eqs. (13.190) and (13.192), we obtain

$$\chi_r = -1/4a = -1/4\alpha(T_c - T), \quad (T < T_c). \tag{13.194}$$

At a constant external field, the specific heat is obtained from the relation

$$C_M = -T\left(\frac{\partial^2 G}{\partial T^2}\right)_h. \tag{13.195}$$

First, we consider the case of zero external field $(h = 0)$. Because $\sigma = 0$ for $T > T_c$,

$$C = C_0 = -Td^2/dT^2 \int g_0(\mathbf{r})d\mathbf{r}, \quad (T > T_c). \tag{13.196}$$

For a uniform system below T_c, it can be shown that (Problem 13.22)

$$G = \int d\mathbf{r}\,[g_0 - (a^2/4b)]. \tag{13.197}$$

Thus, from Eqs. (13.195) and (13.197), the specific heat is

$$C = C_0 + T\int[(\alpha^2/2b) - [\alpha^2(T - T_c)^2/4b^2]db/dT]d\mathbf{r}, \quad (T < T_c). \tag{13.198}$$

Comparing Eqs. (13.196) and (13.198), we note that there is a finite contribution from magnetization to the specific heat just below T_c that results in a finite discontinuity to C at T_c.

PROBLEMS

13.1. Using vector identities, show from Eqs. (13.1) through (13.3) that

$$\mathbf{F} = (\mathbf{m}\times\overrightarrow{\nabla})\times\mathbf{B} = \overrightarrow{\nabla}(\mathbf{m}\cdot\mathbf{B}),$$

where $\mathbf{B}\equiv\mathbf{B}(0)$.

13.2. Show that the induction $\mathbf{B}$ produced by a magnetic dipole of moment $\mathbf{m}_1$ at a distance $\mathbf{r}$, where a second dipole of moment $\mathbf{m}_2$ is located, is given by

$$\mathbf{B} = \overrightarrow{\nabla}\left[\mathbf{m}_1\cdot\overrightarrow{\nabla}\frac{1}{r}\right] = \frac{3\hat{\mathbf{r}}(\mathbf{m}_1\cdot\hat{\mathbf{r}})-\mathbf{m}_1}{r^3}.$$

13.3. From Eqs. (13.8) through (13.10) and Eq. (13.13), show that

$$\varepsilon_{s,t} = <\hat{H}>_{s,t} = 2\varepsilon_0 + \frac{e^2}{R_{12}} + e^2\int d\mathbf{r}_1 d\mathbf{r}_2\,\psi^*_{s,t}(\mathbf{r}_1,\mathbf{r}_2)\left[\frac{1}{|\mathbf{r}_1-\mathbf{r}_2|} - \frac{1}{|\mathbf{r}_1-\mathbf{R}_2|} - \frac{1}{|\mathbf{r}_2-\mathbf{R}_1|}\right]\psi_{s,t}(\mathbf{r}_1,\mathbf{r}_2), \quad (1)$$

where

$$\frac{1}{R_{12}} \equiv \frac{1}{|\mathbf{R}_1-\mathbf{R}_2|}. \quad (2)$$

13.4. From Eqs. (13.14) through (13.17), show that

$$\varepsilon_s = 2\varepsilon_0 + \frac{e^2}{R} + \frac{V_c(R_{12})+V_{ex}(R_{12})}{(1+I^2)} \quad (1)$$

and

$$\varepsilon_t = 2\varepsilon_0 + \frac{e^2}{R} + \frac{V_c(R_{12})-V_{ex}(R_{12})}{(1-I^2)}. \quad (2)$$

13.5. For a two-electron system, we can express

$$\hat{S}_1\cdot\hat{S}_2 = \frac{1}{2}[\hat{S}_1^+\hat{S}_2^- + \hat{S}_2^+\hat{S}_1^-] + \hat{S}_1^z\hat{S}_2^z, \quad (1)$$

where

$$\hat{S}^{\pm} = \hat{S}_x \pm i\hat{S}_y. \quad (2)$$

Show that

$$\hat{S}_1\cdot\hat{S}_2\chi_s = -\frac{3}{4}\chi_s \quad (3)$$

and

$$\hat{S}_1\cdot\hat{S}_2\chi_t = \frac{1}{4}\chi_t, \quad (4)$$

where χ_s and χ_t are the spin singlet and triplet states.

13.6. In the Schwinger representation, the Bose operators are defined as

$$\hat{S}^{\alpha} = \frac{1}{2}\sum_{ii'} \hat{a}_i^{\dagger}\sigma_{ii'}^{\alpha}\hat{a}_{i'}, \tag{1}$$

where σ^{α} are the Pauli spin matrices ($\alpha = x, y, z$). Show from Eq. (1) that

$$\begin{aligned}
\hat{S}^{x} &= \frac{1}{2}(\hat{a}_1^{\dagger}\hat{a}_2 + \hat{a}_2^{\dagger}\hat{a}_1) \\
\hat{S}^{y} &= \frac{1}{2}(\hat{a}_2^{\dagger}\hat{a}_1 - \hat{a}_1^{\dagger}\hat{a}_2) \\
\hat{S}^{z} &= \frac{1}{2}(\hat{a}_1^{\dagger}\hat{a}_1 - \hat{a}_2^{\dagger}\hat{a}_2).
\end{aligned} \tag{2}$$

13.7. By using the Holstein–Primakoff transformation, we have obtained

$$\begin{aligned}
\hat{S}^{+} &= \hat{a}_1^{\dagger}\sqrt{2S - \hat{a}_1\hat{a}_1} \\
\hat{S}^{-} &= \sqrt{2S - \hat{a}_1\hat{a}_1}\,\hat{a}_1 \\
\hat{S}^{z} &= (\hat{a}_1^{\dagger}\hat{a}_1 - S).
\end{aligned} \tag{1}$$

Show that

$$[\hat{S}^{+}, \hat{S}^{-}] = 2\hat{S}^{z}. \tag{2}$$

13.8. In Eq. (13.54), we defined

$$\Phi_m = \hat{S}_m^{-}\Pi_n |S>_n. \tag{1}$$

From Eqs. (13.51) and (13.54), we can write

$$\hat{H}\Phi_m = -J\sum_{ij}{}' \left[\hat{S}_i^{z}\hat{S}_j^{z}\hat{S}_m^{-} + \frac{1}{2}(\hat{S}_i^{+}\hat{S}_j^{-}\hat{S}_m^{-} + \hat{S}_i^{-}\hat{S}_j^{+}\hat{S}_m^{-})\right]\Phi_0. \tag{2}$$

Show by using the commutation relation of the spin operators that

$$\hat{H}\Phi_m = E_0\Phi_m + 2JS\sum_{\mathbf{R}_l}(\Phi_m - \Phi_{m+l}). \tag{3}$$

13.9. Show that the only possible way in which the ground-state energy ε_0 obtained from Eq. (13.59) will be the same as obtained in Eq. (13.53) is to assume $b_i = b_j = b$.

13.10. From Eq. (13.53) and (13.59), show that we can write $\hat{H}$ (up to the first order in S), treating $\hat{a}$ as small, $b = 0$, and multiplying the second term by 2 because $<ij>$ is a sum over nearest-neighbor pairs (each pair appears twice),

$$\hat{H} = -JNzS^2 - 2JS\sum_{<ij>}(\hat{a}_i^{\dagger}\hat{a}_j + \hat{a}_j^{\dagger}\hat{a}_i - \hat{a}_i^{\dagger}\hat{a}_i - \hat{a}_j^{\dagger}a_j). \tag{1}$$

13.11. If all the $\mathbf{R}_i$ vectors are in the A sublattice and the $\mathbf{R}_j$ vectors are in the B sublattice, the spin operators defined in Eqs. (13.40) and (13.42) for ferromagnets can be rewritten for antiferromagnets as

$$\hat{S}_j^z \rightarrow -\hat{S}_j^z \tag{1}$$

and

$$\hat{S}_j^{\pm} \rightarrow \hat{S}_j^{\mp}. \tag{2}$$

Show that the Hamiltonian in Eq. (13.51) for ferromagnets can be rewritten for antiferromagnets as

$$\hat{H} = 2|J| \sum_{<ij>} \left[-\hat{S}_{iz}\hat{S}_{jz} + \frac{1}{2}(\hat{S}_i^+ \hat{S}_j^+ + \hat{S}_i^- \hat{S}_j^-) \right]. \tag{3}$$

13.12. Using a procedure adapted to obtain Eq. (13.57) with the modifications for antiferromagnets (Eqs. 13.68 through 13.70), show that

$$\begin{aligned} \hat{H} = 2|J| \sum_{<ij>} \Bigg[& -(S - \hat{a}_i^\dagger \hat{a}_i)(S - \hat{a}_j^\dagger \hat{a}_j) + \frac{1}{2}\hat{a}_i^\dagger \sqrt{2S - \hat{a}_i^\dagger \hat{a}_i}\, \hat{a}_j^\dagger \sqrt{2S - \hat{a}_j^\dagger \hat{a}_j} \\ & + \frac{1}{2}\sqrt{2S - \hat{a}_i^\dagger \hat{a}_i}\, \hat{a}_i \sqrt{2S - \hat{a}_j^\dagger \hat{a}_j}\, \hat{a}_j \Bigg]. \end{aligned} \tag{1}$$

13.13. By following a $1/S$ expansion method similar to the procedure outlined in Eqs. (13.59) and Eq. (13.70), derive from Eq. (1) of Problem 13.12

$$\hat{H} = -|J|NzS^2 + 2|J|S \sum_{<i,j>} [\hat{a}_i^\dagger \hat{a}_i + \hat{a}_j^\dagger \hat{a}_j + \hat{a}_i^\dagger \hat{a}_j^\dagger + \hat{a}_i \hat{a}_j]. \tag{1}$$

13.14. We derived

$$\hat{H} = -|J|NzS^2 + |J|S| \sum_{\mathbf{k},l} [2\hat{b}_{\mathbf{k}}^\dagger \hat{b}_{\mathbf{k}} + (\hat{b}_{\mathbf{k}}^\dagger \hat{b}_{-\mathbf{k}}^\dagger + \hat{b}_{\mathbf{k}} \hat{b}_{-\mathbf{k}}) \cos(\mathbf{k} \cdot \mathbf{R}_l)], \tag{1}$$

where $\mathbf{R}_l$ are nearest-neighbor vectors. To diagonalize the Hamiltonian, we introduced two new operators through the transformation,

$$\hat{b}_{\mathbf{k}} = (\sinh \beta_{\mathbf{k}})\, \hat{c}_{-\mathbf{k}}^\dagger + (\cosh \beta_{\mathbf{k}})\, \hat{c}_{\mathbf{k}}, \tag{2}$$

where β is real. Show that by substituting Eq. (2), the Hamiltonian in Eq. (1) is diagonalized provided

$$\tanh 2\beta_{\mathbf{k}} = -\frac{1}{z} \sum_l \cos(\mathbf{k} \cdot \mathbf{R}_l). \tag{3}$$

13.15. Derive from Eqs. (13.88) and (13.91) that the ratio of saturation magnetization $M(T)$ at temperature T and $M(0)$ at zero temperature is

$$\frac{M(T)}{M(0)} = 1 - \frac{1}{S} e^{-3T_C/(S+1)T}. \tag{1}$$

13.16. The chemical potential is the same for the two electron distributions with up- and down-spins. Show that, to satisfy this, the following conditions have to be met:

$$n<\mu> = \mu_B \int_0^\infty \frac{1}{2}\{f^0(\varepsilon_{\mathbf{k}\uparrow}) - f^0(\varepsilon_{\mathbf{k}\downarrow})\} D(\varepsilon) d\varepsilon \tag{1}$$

and

$$n = \int_0^\infty \frac{1}{2}\{f^0(\varepsilon_{\mathbf{k}\uparrow}) + f^0(\varepsilon_{\mathbf{k}\downarrow})\} D(\varepsilon) d\varepsilon. \tag{2}$$

13.17. We derived in Eq. (13.135)

$$\hat{H} = \sum_{<ij>,\rho} -t[\hat{a}_{i\rho}^\dagger \hat{a}_{j\rho} + \hat{a}_{j\rho}^\dagger \hat{a}_{i\rho}] + U\sum_i (\hat{n}_{i\uparrow} n_\downarrow + n_\uparrow \hat{n}_{i\downarrow} - n_\uparrow n_\downarrow). \tag{1}$$

Making a Fourier transformation of the type

$$\hat{a}_{i\rho} = \frac{1}{\sqrt{N}} \sum_{\mathbf{k}} e^{i\mathbf{k}\cdot\mathbf{R}_i} \hat{b}_{\mathbf{k}\rho}, \tag{2}$$

show that

$$\hat{H} = \sum_{\mathbf{k},\mathbf{R}_l,\rho} -t\hat{b}_{\mathbf{k}\rho}^\dagger \hat{b}_{\mathbf{k}\rho} \cos \mathbf{k}\cdot\mathbf{R}_l + U\sum_{\mathbf{k}} (\hat{n}_{\mathbf{k}\uparrow} n_\downarrow + n_\uparrow \hat{n}_{\mathbf{k}\downarrow} - n_\uparrow n_\downarrow). \tag{3}$$

13.18. We derived in Eq. (13.145)

$$H'(\mathbf{k}, \xi_l) = -ih_{\alpha\beta}\Pi^\alpha \nabla_{\mathbf{k}}^\beta + \frac{1}{2} g\mu_B B^\mu \sigma^\mu + B^\mu \Sigma^{1,\mu}(\mathbf{k}, \xi_l). \tag{1}$$

Here, $\overrightarrow{\Pi}$ was defined in Eq. (12.133),

$$\overrightarrow{\Pi} = \frac{\hbar}{m}(\mathbf{p} + \hbar\mathbf{k}) + \frac{\hbar^2}{4m^2c^2} \overrightarrow{\sigma} \times \overrightarrow{\nabla} V + \nabla_{\mathbf{k}} \Sigma^0(\mathbf{k}, \xi_l). \tag{2}$$

In addition, from Eqs. (13.147) and (13.148), we have

$$\widetilde{G}(\mathbf{k}, \xi_l) = G_0(\mathbf{k}, \xi_l) + G_0(\mathbf{k}, \xi_l)\hat{H}' G_0(\mathbf{k}, \xi_l) + \cdots \tag{3}$$

and

$$\nabla_{\mathbf{k}}^\alpha G_0(\mathbf{k}, \xi_l) = G_0(\mathbf{k}, \xi_l)\, \Pi^\alpha G_0(\mathbf{k}, \xi_l). \tag{4}$$

From Eqs. (1) through (4), show that

$$\widetilde{G}(\mathbf{k}, \xi_l) = G_0 - G_0 \left[ih_{\alpha\beta}\Pi^\alpha \nabla_{\mathbf{k}}^\beta - \frac{1}{2} g_0 \mu_B B^\nu F^\nu \right] G_0, \tag{5}$$

where

$$F^\nu = \sigma^\nu + \frac{2}{g\mu_B} \widetilde{\Sigma}^{1,\nu} \tag{6}$$

was defined in Eq. (12.147) and is the renormalized spin vertex of the electron–electron interaction.

13.19. From Eqs. (12.123) and (13.149), the quasiparticle contribution to the thermodynamic potential is obtained. After evaluating the trace and contour integration, show that

$$\Omega_{qp} = \frac{1}{2}\mu_B B^v \sum_{n\mathbf{k}\rho m\rho',m\neq n}\left[gF^v_{n\rho,n\rho'} + \frac{ie}{\hbar c\mu_B}\in_{\alpha\beta v}\frac{\Pi^\alpha_{n\rho,m\rho'}\Pi^\beta_{m\rho',n\rho}}{E_{mn}}\right]f(E_{n\mathbf{k}\rho}), \tag{1}$$

where $f(E_{n\mathbf{k}\rho})$ is the Fermi distribution function for an electron in band n and spin ρ,

$$\Pi^\alpha_{n\rho,m\rho'} = \int_{cell} d^3r u^*_{n\mathbf{k}\rho}\Pi^\alpha u_{m\mathbf{k}\rho'} \tag{2}$$

and

$$E_{mn} = E_m(\mathbf{k}) - E_n(\mathbf{k}). \tag{3}$$

13.20. The contribution of correlation to magnetization is

$$M^v_{corr} = -\frac{\partial\Omega_{corr}}{\partial B^v} = \frac{1}{\beta}Tr\,\frac{\partial\widetilde{\Sigma}_{\xi_l}}{\partial B^v}\widetilde{G}_{\xi_l}. \tag{1}$$

Simplifying Eq. (1) with the use of Eqs. (12.127), (12.128), (13.145), (13.147), and the Luttinger–Ward (Ref. 16) prescription for frequency summation,

$$\frac{1}{\beta}\sum_{\xi_l}\frac{1}{(\xi_l - \hat{H}_0)^m} = \frac{1}{2i\pi}Tr\int_{\Gamma_0}\frac{1}{(\xi - \hat{H}_0)^m}f(\xi)\,d\xi, \tag{2}$$

where Γ_0 encircles the real axis in a clockwise direction, and $f(\xi)$ is the Fermi distribution function, show that

$$M^v_{corr} = \sum_{n\mathbf{k}\rho}\widetilde{\Sigma}^{1,v}_{n\rho,n\rho'}f(E_{n\mathbf{k}\rho}). \tag{3}$$

13.21. The many-body Hamiltonian can be written as

$$\hat{H}_0 = \sum_{\mathbf{k}\rho}\varepsilon_{\mathbf{k}}c^\dagger_{\mathbf{k}\rho}c_{\mathbf{k}\rho} + \frac{1}{2}\sum_{\mathbf{qkk}'\rho\rho'}V(\mathbf{q})c^\dagger_{\mathbf{k}+\mathbf{q},\rho}c^\dagger_{\mathbf{k}'-\mathbf{q},\rho'}c_{\mathbf{k}',\rho'}c_{\mathbf{k},\rho}, \tag{1}$$

where $c^\dagger_{\mathbf{k}\rho}$ and $c_{\mathbf{k}\rho}$ are the creation and annihilation operators for an electron with wave vector $\mathbf{k}$ and spin ρ, and $V(\mathbf{q})$ is the Fourier transformation of the Coulomb interaction. $E_{\mathbf{k}\rho}$ can be obtained by using the mean-field approximation,

$$E_{\mathbf{k}\rho} = \frac{1}{N}\left\langle\left\{[c_{\mathbf{k}\rho},\hat{H}_0],c^\dagger_{\mathbf{k}\rho}\right\}\right\rangle. \tag{2}$$

From Eqs. (1) and (2), show that

$$E_{\mathbf{k}\rho} = \varepsilon_{\mathbf{k}} - \frac{1}{N}\sum_{\mathbf{q}} V(\mathbf{q}) f(\varepsilon_{\mathbf{k}-\mathbf{q},\rho}) + \frac{1}{N} V(0) \sum_{\mathbf{k}} [f(\varepsilon_{\mathbf{k}\rho}) - f(\varepsilon_{\mathbf{k},-\rho})]. \tag{3}$$

13.22. Show that for a uniform system below T_c,

$$G = \int d\mathbf{r}[g_0 - (a^2/4b)]. \tag{1}$$

Hence, show by using Eq. (13.195) that the specific heat is

$$C = C_0 + T\int [(\alpha^2/2b) - [\alpha^2(T - T_c)^2/4b^2] db/dT] d\mathbf{r}. \quad (T < T_c) \tag{2}$$

References

1. Anderson PW. Localized magnetic states in metals. *Phys Rev* 1961;**124**:41.
2. Ashcroft NW, Mermin ND. *Solid state physics*. New York: Brooks/Cole; 1976.
3. Callaway J. *Quantum theory of the solid state*. New York: Academic Press; 1976.
4. Gunnarson O. Band model for magneticism of transition metals in the spin-density-funcional formalism. *J Phys F, Met Phys* 1976;**6**:587.
5. Heisenberg W. On the theory of ferromagnetism. *Z Physik* 1926;**49**:619.
6. Heitler W, London F. Interaction of neutral atoms and homopolar binding in quantum mechanics. *Z Physik* 1927;**44**:455.
7. Holstein T, Primakoff H. Field dependence of the intrinsic domain magnetization of a ferromagnet. *Phys Rev* 1940;**58**:1098.
8. Hubbard J. Electron correlations in narrow energy bands. *Proc R Soc Lond* 1963;**A277**:237.
9. Janak JF. Uniform susceptibilities of metallic elements. *Phys Rev B* 1976;**16**:255.
10. Kasuya T. A theory of metallic ferro- and antiferromagnetism on Zener's model. *Prog Theor Phys (Kyoto)* 1956;**16**:45.
11. Kittel C. *Introduction to solid state physics*. New York: John Wiley & Sons; 1976.
12. Kittel C. *Quantum theory of solids*. New York: John Wiley & Sons; 1987.
13. Kittel C. *Indirect Exchange Interaction in Metals. Solid State Phys* 1968;**22**:1.
14. Kondo J. Resistance minimum in dilute magnetic alloys. *Prog Theor Phys* 1964;**32**:37.
15. Landau LD. On the theory of phase transition. *Phhysikalliische Zeitschraft der Sowjetunion* 1937;**11**:26 and 545.
16. Luttinger JM, Ward JC. Ground-state energy of a many fermion system II. *Phys. Rev.* 1960;**118**:1417.
17. Marder MP. *Condensed matter physics*. New York: John Wiley & Sons; 2000.
18. Misra SK, Misra PK, Mahanti SD. Many-body theory of magnetic susceptibility of electrons in solids. *Phys Rev B* 1982;**26**:1903.
19. Misra PK, series editor, Blackman J, editor. *Metallic nanoparticles*. Amsterdam: Elsevier; 2008.
20. Nagaoka Y. Self-consistent treatment of Kondo effect in dilute alloys. *Phys Rev* 1965;**138**:A1112.
21. Neel L. Magnetic properties of ferrites: Ferromagnetism and sntiferromagnetism. *Annales de Physique* 1948;**3**:137.
22. Rado GT, Suhl H, editors. *Magnetism*. New York: Academic Press; 1963.
23. Ruderman MA, Kittel C. Indirect exchange coupling of nuclear magnetic moments by conduction electrons. *Phys Rev* 1954;**96**:99.
24. Schwinger J. *Quantum theory of angular momentum*. New York: Academic Press; 1965.

25. Stoner EC. *Magnetism in matter*. London: Methuen; 1934.
26. Stoner EC. Collective electron ferromagnetism II. Energy and specific heat. *Proc R Soc Lond A* 1939;**169**:339.
27. Stoner EC, Wohlfarth EP. A Mechanism of Magnetic Hysteresis in Heterogeneous Alloys. *Phil Trans Lond A* 1948;**240**:599.
28. Tripathi GS, Das LK, Misra PK, Mahanti SD. Theory of spin-orbit and many-body effects on the Knight shift. *Phys. Rev. B* 1982;**25**:3091.
29. Tripathi GS, Misra PK. Many-body theory of magnetization of Bloch electrons in te presence pf spin-orbit interaction. *J Magn Mag Mater* 2010;**322**:88.
30. Vosko SH, Pedrew V. Theory of the spin susceptibility of an inhomogeneous electron gas via the density functional formalism. *Can J Phys* 1975;**53**:1385.
31. Yosida K. Many-body theory of magnetization of Bloch electrons in the presence of spin-orbit interaction. *Phys Rev* 1957;**106**:893.
32. Ziman JM. *Principles of the theory of solids*. Cambridge: Cambridge University Press; 1972.